AN APPLICATION OF FEM TO THE STUDY OF ASPERITY JUNCTIONS IN ADHESIVE WEAR

A Thesis Submitted

In Partial Fulfilment of the Requirements

for the Degree of

MASTER OF TECHNOLOGY

by

B. V. BALIGA

to the

DEPARTMENT OF MECHANICAL ENGINEERING

INDIAN INSTITUTE OF TECHNOLOGY KANPUR

AUGUST, 1986

Dedicated to

MY FATHER

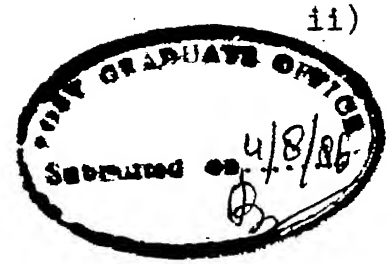

CERTIFICATE

This is to certify that the work entitled, "AN APPLICATION OF FEM TO THE STUDY OF ASPERITY JUNCTIONS IN ADHESIVE WEAR" by B.V. Baliga has been carried out under our supervision and has not been submitted elsewhere for a degree.

Dr.M.K. Muju
Assistant Professor
Department of Mech. Engg.
Indian Institute of Technology
Kanpur

Dr. N.N. Kishore
Assistant Professor
Department of Mech. Engg.
Indian Institute of Technology
Kanpur

August, 1986.

ACKNOWLEDGEMENTS

I am extremely grateful to Dr. M.K. Muju and Dr. N.N. Kishore for their inspiring guidance, invaluable suggestions, constructive critisms, invaluable suggestions and for being a constant source of encouragement through out this work.

I am also thankful to Mr. P.B. Poppat for his invaluable suggestions during this work. I am thankful to my friends Pankaj and Ravi for their constant support and encouragement. I am also very grateful to all my friends who made my stay here a very pleasant one.

A special word of thanks at this stage for Mr. U.S. Mishra for his careful and efficient typing work and Mr. Gopal for his cyclostyling of the manuscript.

I am deeply indebted to my mother and brothers for their loving support and encouragement in my pursuit for masters degree.

At the end I am thankful to all those who helped me directly or indirectly during my stay at I.I.T. Kanpur.

August, 1986 -B.V. Baliga

CONTENTS

LIST OF FIGURES

NOMENCLATURE

$\underline{a}^e$	nodal displacement vector for a particular element
$[B]$	strain-displacement matrix
$[D]$	stress strain matrix
$[\bar{D}_p]$	plastic stress strain matrix
$[\bar{D}_{ep}]$	elastic-plastic matrix
E	elastic modulus
f	coefficient of friction
$\bar{F}_1$	average instantaneous values of shear force
F_1	instantaneous shear force on asperity junction
H	strain hardening parameter
$[J]$	Jacobian matrix
$\|J\|$	determinant of jacobian
$[\bar{K}]$	global stiffness matrix
$[K_E]$	elemental stiffness matrix
L_1, L_2, L_3	natural coordinates for triangular element
N	contact load
$\bar{N}_1$	average instantaneous values of normal force
N_1	instantaneous normal force on asperity junctions
NEL	total number of elements
N_i	shape function
P_1	mean normal stress (compressive)
$\{Q\}$	global load vector
$\{R_i\}$	nodal force vector
S_1	tangential stress (shear)
t	thickness

u	nodal displacement in x direction
v	nodal displacement in y direction
w_1, w_2, w_3	weights for gaussian integration
Z	wear coefficient

Greek

ϕ	approach angle
ε	strain
σ	stress
ε_o	initial strain
σ_o	initial stress
ν	Poissons ratio
$\sigma_1, \sigma_2, \sigma_3$	principal stress
σ_{yp}	tensile yield stress
σ'_x, σ'_y	deviatoric stress (components x and y direction)
τ_{xy}	shear stress

SYNOPSIS

A Thesis Submitted
In partial fulfillment of the requirements
for the degree
of

MASTER OF TECHNOLOGY

by

B. VISHWANATH BALIGA
Department of Mechanical Engineering
Indian Institute of Technology, Kanpur
AUGUST, 1986

The present work is an attempt to analyse fracture in a welded asperity junction. The welded asperity junction is formed during rubbing motion between two surfaces, wherein the high points of the surfaces come in contact with each other and due to the intense local stresses a strong welded junction of these asperities (high points) is formed. Adhesive wear, has been found to occur when these junction formed fracture. While reviewing the available literature it was found that no exact analytical work on the formation of a wear particle as a result of fracture of asperity junction has been done. A few experimental results are available wherein the path of fracture of these junctions have been analysed.

The finite element method was applied to this present analysis because it is a versatile method and it can easily accommodate material non-linearity, geometric non-linearity and complex boundary conditions when compared with numerical

methods. Based on the displacement formulation, an elastic analysis computer code using FEM is developed to predict the path of fracture in a brittle junction. Also, a ductile junction was analysed for the fracture path using a elasto-plastic analysis computer code based on the initial stress method. Material was considered to obey Von-Mises yield criterion. Six node isoparametric elements are used in the discretization of the continuum.

The junction is analysed at a stage in its formation, where it is perfectly symmetric and the fracture is just about to start. A fracture path is traced with the fracture occurring in only one of the asperities as happens in a bimetallic junction. Fracture path is also traced with the fracture occurring in both the asperities simultaneously as is the likely case in junctions of similar metals. Three different finite element meshes are used to reach the path of fracture.

CHAPTER 1

INTRODUCTION TO THE ADHESION WEAR

1.1 Introduction:

The study of wear due to the fracture of minute asperities resulting from large plastic deformations of welded asperity junctions formed on the sliding surfaces has been investigated by several research workers in this area. These welded asperity junctions are formed between the two metals wherever asperities engage and these junctions adhere strongly under intense local stresses. Each one of these welded asperity junctions goes through a life cycle; formation, plastic deformation and eventually fracture; new junctions being formed as fast as the old ones are fractured.

The problem of fracture is the central problem in the Science of resistance of materials. At present when speaking of fracture one usually implies a study of the conditions under which there is a crack or a system of cracks propagating in a body. But cracks may be very different in nature and they are considered on different scales. On one hand, the fracture of a crystal grain begins with the formation of a submicroscopic crack with the separation of two atomic layers by such a distance that the force of interaction between the atoms are zero. On the other hand we have the macroscopic crack (as in the case of welded turbine rotor or in a nuclear reactor) where the length and width of the crack may be estimated by the milimetre.

The fundamental problem on which most investigators have concentrated in recent years has been the problem of finding the conditions for the propagation of a crack. The propagation of the crack begins, when the plastic strain near its tip becomes large. The criterion for the initiation of crack propagation, which forms the basis of fracture mechanics does not follow from the equilibrium equations, but is an additional boundary condition in the solution of the problem. Fracture condition is said to be reached if a crack like cut can propagate [1].

The study of crack propagation has been done by several research workers using numerical techniques. At present one of the most generally used method, having the least limitations is the finite element method. In the last few years the finite element method has found extensive application in the solution of various complex problems in structural mechanics, elasticity and other fields. In many situations an adequate engineering model of the system is obtained by replacing the system with a finite number of well defined components called elements. Even if the number of elements is very large the problem can now be solved readily with the advent of computers. The various discretization methods suggested from time to time to solve the continuum problem involve approximations which approach the true continuum solution as the number of discrete variables increase.

Finite element method can be interpreted as a piecewise application of the variational methods, in which the approximation functions are algebraic polynomials and the undetermined parameters represent the values of the solution of a finite number of preselected points called nodes; on the boundary and in the interior of the element. Finite element method can thus be systematically programmed to accommodate complex, non-linear stress - strain behaviour and complex boundary conditions which will be very difficult to accommodate in other numerical methods like the method of least squares, Ritz method etc.

1.2 Review of Previous Work:

(a) On Asperity Junction:

It is a well established fact that when two solid bodies, in contact, are in the relative sliding motion, surface deterioration invariably occurs. The surface deterioration ultimately leads to wear of these bodies. Because of the waviness and roughness of surfaces, contact between two sliding bodies (Fig. 1.1) occurs only at certain high points known as asperities. These asperities are subjected to very high stresses even at small loads due to their small dimensions. Due to the high stresses contact of the two bodies at the asperities generally results in the formation of welded asperity junctions, which have been the subject of investigation for many research workers. Various experimental

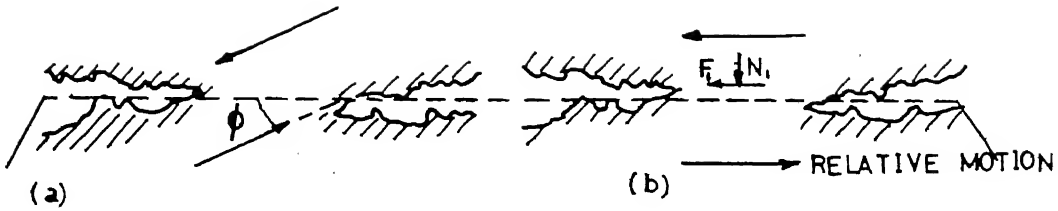

FIG 1.1 DIAGRAM OF A JUNCTION (a) DURING THE INITIATION OF SLIDI
(b) DURING STEADY SLIDING

techniques like electrical resistance measurements [8,9], optical [10] have been carried out, based on these it is generally accepted that the junctions formed by the asperity interactions are roughly of the order of 10 to 20μ .

Rabnowicz [11] used an auto-correlation analysis to determine the average junction size for sliding metals. The size distribution of the junctions is given in Fig.1.2.

Green [12] has modelled as asperity junction (Fig.1.3). At any instant when the junction is formed, force acting through the junction has a normal component N_1 (compressive) and a tangential force F_1 (shear) as shown in Fig. 1.3. Brockley and Fleming [13] have conducted experimental work on a model junction simulating metallic wear. They have predicted the wear rate by dividing the volume of the detached particle formed to the distance traversed during a particular deformation. Fig. 1.4 shows how the fracture starts during the process of sliding and plastic deformation.

Literature survey conducted by the author did not reveal any Finite Element application to wear analysis. As already mentioned, the formation of a wear particle during adhesive wear is a complex phenomena. No exact analytical work to estimate the amount of material that can get lost by a solid during the interaction with another body has been done. However, a large number of empirical equations have been given. Only Green [14] and Brockley [13] have discussed the formation of a wear particle by tracing the fracture path

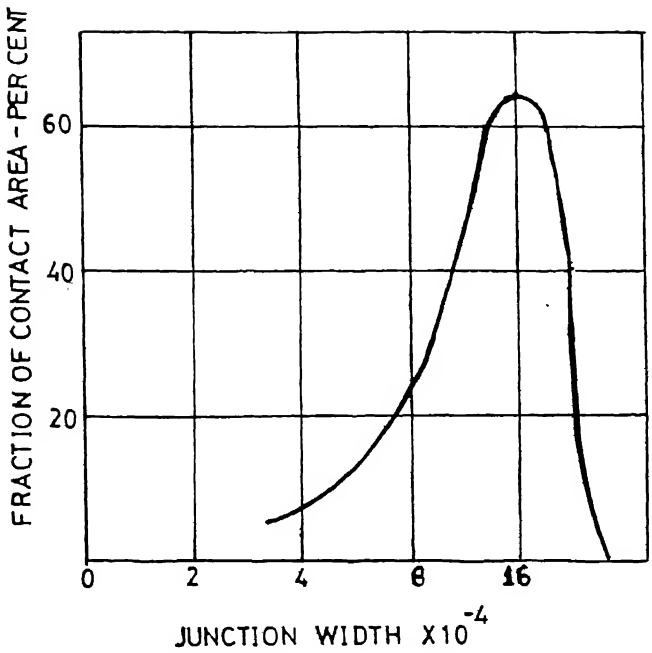

FIG 1.2 FRACTION OF CONTACT AREA AS A FUNCTION OF JUNCTION WIDTH

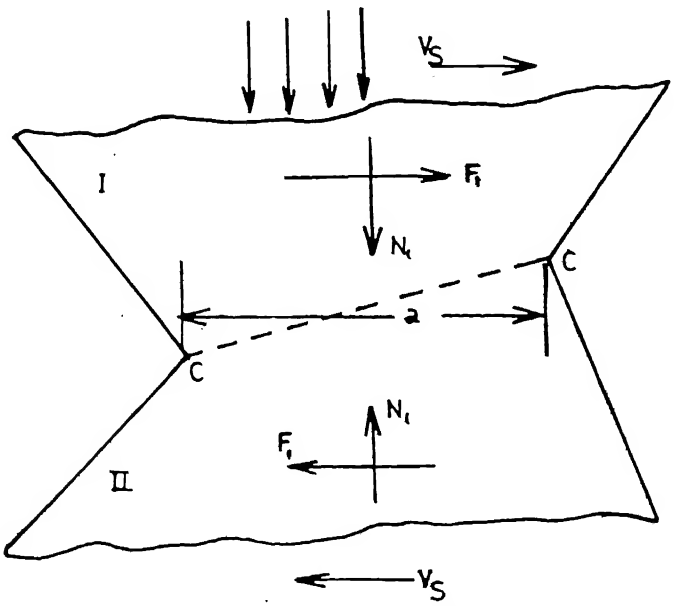

FIG 1.3 MODEL OF AN ASPERITY JUNCTION

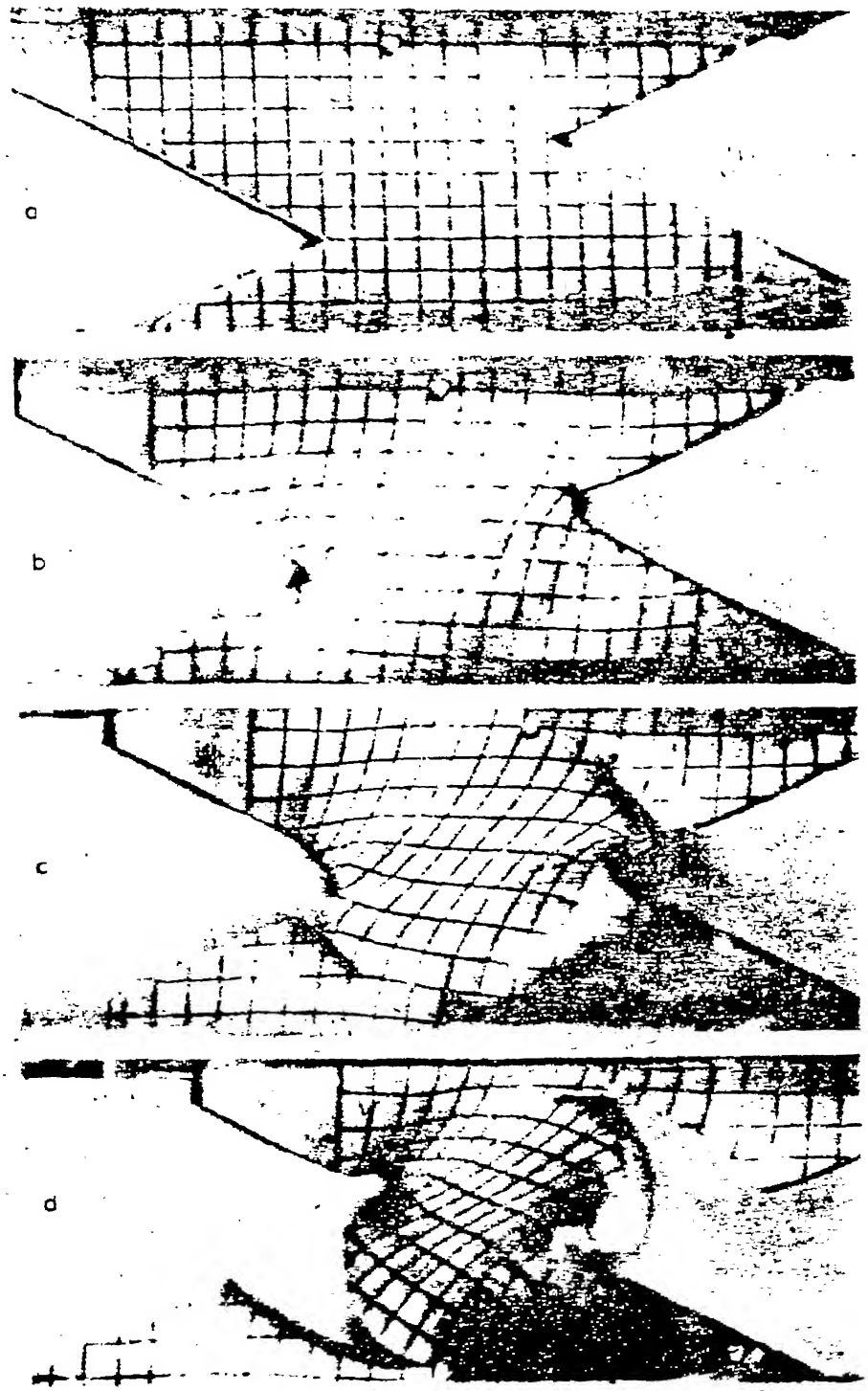

Fig. 1.4 : Crack Path in Unimetallic Junction

at a interface. Green discusses it only for a perfectly plastic material, Brockley through experiments has shown how a wear particle can be formed.

(b) On Fracture:

The importance of fracture mechanics for the study of crack propagation and its effects in structures has increased considerably over the recent years. A factor known as the stress intensity factor, K, has been developed as the critical value for crack to propagate. The magnitude of K depends on the structural geometry and the loading system. If the value of K exceeds a certain critical valuel, K_c, crack instability is assumed to exist, so that K_c is now effectively a material property which represents the resistivity of the material to fracture [1].

A number of solutions for K, have been deduced for various crack sizes and loading for relatively simple shaped structures, Paris and Sih [2] give a comprehensive handbook of such results. However, for more realistic complex shapes encountered in practice more general techniques are required. Use of Finite Element Method enables such computations to be made. Jerram and Hellen [3], using finite element have derived stresses and displacements around the crack tip and then using the computed values have evaluated K. The computed values of stresses and displacements substituted into the known crack tip field equations which relate stress and

displacement to K, yield the value for the stress intensity factor.

Watwood [4] has done considerable work based on the energy release criteria of Griffiths [5] using this method Watwood and others have calculated the energy differences between successive points along a mesh representing a growing crack and used this to find the possible path of fracture. This method is sometimes referred to as virtual crack extension method [6].

A different method has been developed by Parks [7]. He uses the J-integral approach on a piecewise straight path around the crack tip along the sides of the element used. Parks [7] has also shown that using a constant stress triangle el the virtual crack extension method is equivalent to the J-integral approach when expressed in terms of stresses and displacements.

1.3 Junction Formation between Contacting Bodies:

No matter how plane the surface of a solid may appear to be, when examined at microscopic level it is always wavy and rough. The length of the waves varies from 1 mm - 10 mm and their heights vary from 20-50μ [14]. A profile of a actual surface is shown in Fig. 1.5 [15]. Due to this distortions in shape, the actual surfaces are in a position to develop contact only over small discrete areas.

FIG. 1.5 ROUGHNESS AND WAVINESS OF SURFACES

(A.) PROFILE OF A TURNED COPPER SURFACE (TOP) DISTORTED MAGNIFICATION (BELOW) EQUAL MAGNIFICATI
(B.) WAVINESS DIAGRAM OF A TURNED SURFACE

A closer examination of these discrete regions of contact has revealed further that the actual contact between bodies occurs at certain high points located within these regions, these regions are called as contact points or more commonly asperities. Problems connected with metal transfer and wear during sliding process are very much dependent on the nature of phenomenae taking place at these contact asperities. These asperities are subjected to extremely high stresses even at ordinary loads, because of their very small dimensions. Due to the high stresses contact of the two bodies at the asperities generally results in formation of junctions which have been the subject of investigations for many research workers. Various experimental techniques like electrical resistance measurement [16, 17], optical [18] and electron microscopy [19] have been employed to study these asperity junctions.

Rabinowitz proposes the size distribution of the junction to be given as in Fig. 1.2. Ling [20], Greenwood and Willamson [21] and many others have also analysed surface profiles using statistical approaches and have generally concluded that the junction size varies from 5–20 μ under normal conditions of rubbing.

Adhesive Wear:

The tendency of the contacting surfaces to adhere arises from the attractive forces which exist between the surface atoms of the two materials. If two surfaces are brought together and then separated, either normally or

tangentially, the attractive forces act in such a way as to attempt to pull material from one surface on to the other. Whenever, material is removed from its original surface in this way an adhesive wear fragment is created. The strength of bonding at the points of adhesion is sometimes so great that while attempting to free the surfaces separation takes place not along the interface but in one of the bodies itself resulting in metal transfer and subsequent metal removal, this will occur if the force required to break through the interface of the materials is larger than the force required to break through some continuous surface inside one of the materials. It has been experimentally observed that because of the intense local stresses at the junction, strong adhesion generally occurs at the interface and hence fracture takes place mostly along some continuous path inside one of the materials. Thus under some conditions, loss of material may occur from one or from both of the rubbing pair. This type of wear is called as adhesive wear. This is the most common form of metal wear and exists predominantly at moderate cutting conditions. The removal of material takes place in the form of small particles which are generally transferred to the other surface but may also come of in loose form.

The way in which wear particles form is graphically illustrated by the experiments of Green [12] who used two-dimensional models of various metals and plasticene to denote

asperities, and then sheared the asperities.

The stages through which junctions have been observed to be passing can be understood with the aid of Fig. 1.6. The figure illustrates the deformation of asperities I and II of similar hardness. After the initial adhesion most of the centre of the junction is sheared uniformly; Fig.1.6(c). Due to this shearing the interface gets stretched. This would help to break any surface films present and thereby strengthen adhesion. As the tendency for the asperities to pass each other continues an intermediate stage shown in Fig.1.6(d) is reached when the junction has acquired a symmetric shape. Since the adhesion is assumed to be fairly strong the junction deforms as a single body and thus necking and fracture occurs in the most critically stressed region of the junction. In this manner a small particle is transferred from one asperity to the other one. In a subsequent encounter this transferred material may become a loose wear fragment.

Experiments have shown that most of the times the softer asperity looses material to the harder one but the probability of harder body loosing material is also finite. The reason for this is the presence of weak spots within the harder asperity as well as its fatigue caused by the interactions. In general, therefore, the fracture occurs more often on the side of the softer asperity as against that of the harder asperity.

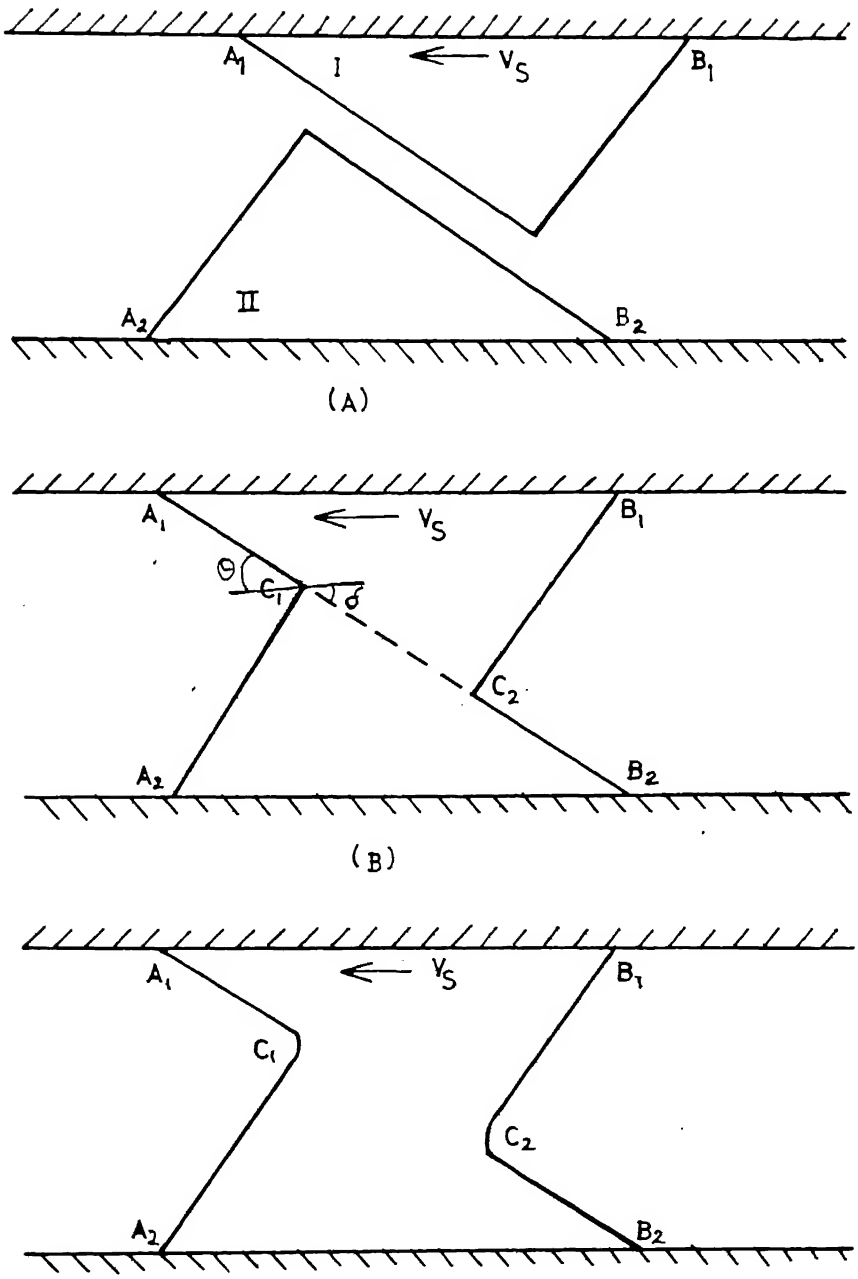

FIG 16 (CONTD.)

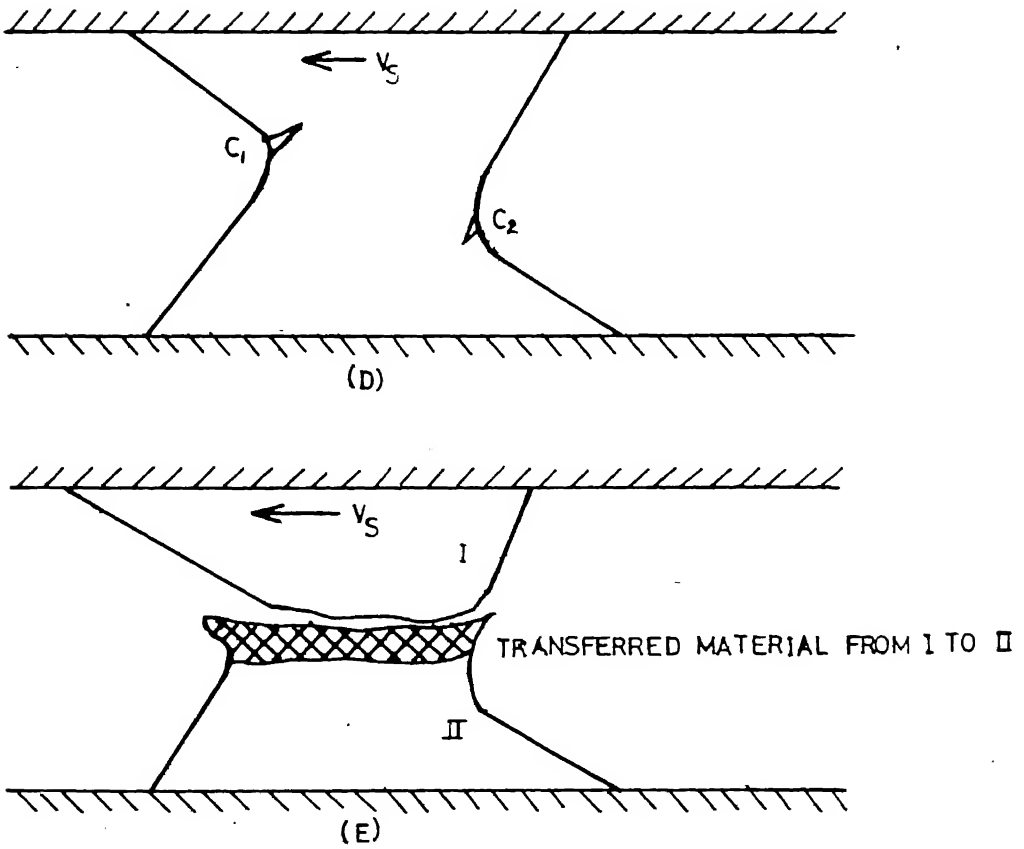

FIG 1.6 FRACTURE OF A SLIDING ASPERITY JUNCTION

Brockley and Fleming [13] conducted the experiments on copper metallic junctions cut from one piece. These single piece junctions were made to shear by applying a load from a motor. They studied the failure of these junctions in detail. The failure of these junctions is shown in Fig.1.4. The figure illustrates that a junction formed by two identical materials has equal probability of failure on either side of the interface. This figure also indicates that compression, rotation, tension and shearing at the ends of the junctions are apparently involved in the process. Thus the mechanism of wear fragment formation is quite complex and does not render itself to convenient analytical solution. However rough estimates of the forces exerted through such junctions have been attempted by Green [14], Edward and Halling [22], and Gupta and Cook [23].

Now let the Fig.1.6(a), where the asperities have just met, be considered. A mean normal stress (compressive) P_1 and a tangential (shear) stress S_1 act through the junction. Due to these stresses the junction is deformed so that the two surfaces move parallel to one another. These stresses calculated by Green [14] are shown in Fig.1.7. For normal values of surface roughness, angles δ_1 and θ_1 shown in Fig.1.3 are less than 10°, when a junction is formed. For such values of δ_1 and θ_1 it can be seen from Fig. 1.7 that $S_1 \simeq 1.25\ K_1$ and $P_1 \simeq 2\ K_1$, where K_1 represents the yield stress in shear of the softer body. Further deformation

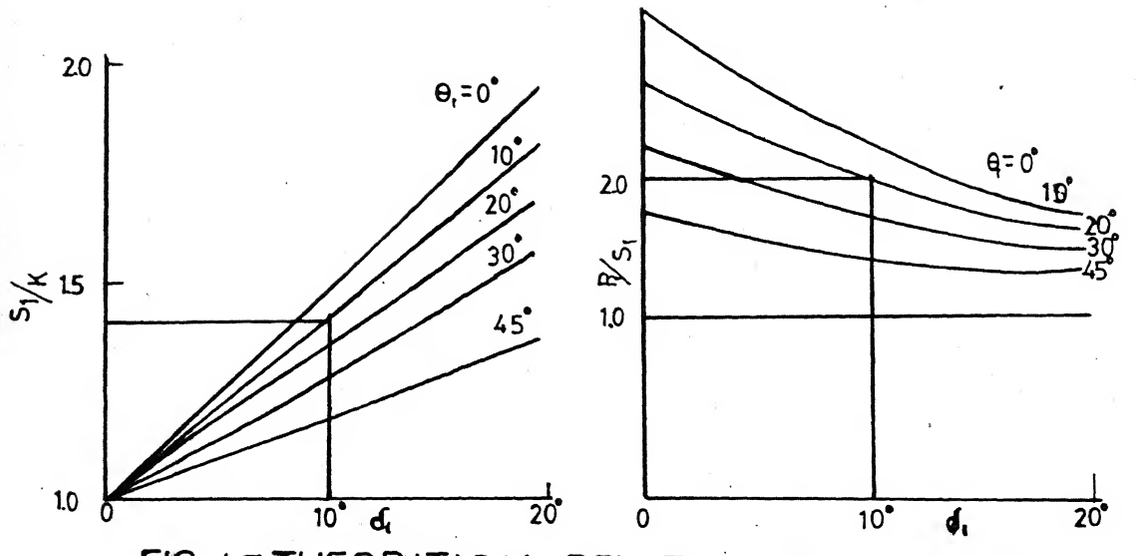

FIG. 1.7 THEORITICAL RELATIONS FOR STRONG JUNCTIONS BETWEEN S/K AND α_1, P/S_1 AND α_1 FOR VARIOUS VALUES OF θ.

as shown in Fig.1.6(c) and Fig.1.6(d), causes changes of shape such that θ_1 increases δ_1 decreases. It is also seen from Fig.1.7 that as δ_1 decreases and θ_1 increases S_1 tends to K_1 and P_1 decreases continuously. Also as the junction tends to become roughly symmetrical P_1 continues to decrease. Thus, when the junction has been deformed to the symmetrical state the normal stress on it is zero and the tangential stress is nearly equal to its initial value. After the symmetrical shape has been achieved the cycle gets reversed, i.e. S_1 increases slightly while P_1 becomes tensile and remains so until the junction eventually breaks under combined shearing and tensile forces. Thus after the asperities have matched up and firmly welded the cross section 'a' remains approximately constant until necking and fracture commences.

The formation of a loose wear particle can be understood to occur as a result of the following stages:

(a) Matching up of two asperities

(b) Adhesion of these asperities across the interface

(c) Fracture initiation at a critical point

(d) Transfer of material from one asperity to another, and

(e) Subsequent disintegration and removal of this transferred material.

1.4 Objective and Scope of Present Work:

In this present work an attempt has been made to find the path of fracture at welded asperity junction formed during adhesion of two bodies in sliding contact. The path has been obtained using finite element analysis of the junction. Since FEM is a powerful technique, it was considered that it could be applied to fracture of asperity junction. The possible advantage could be that FEM can easily account for material nonlinearity, different geometries of the asperity junction and complex boundary conditions.

The present work is basically divided in two stages. The path of fracture for two different kinds of asperity junctions has been studied, (1) For a brittle material junction wherein the fracture takes place instantly without the junction going into the plastic deformation stage. This analysis was done using elastic analysis of finite element technique. (2) For a ductile material junction wherein large plastic deformations occur before fracture. Here the Elasto-Plastic Analysis of Finite Element Technique was used. This non-linear analysis was done using the initial stress method.

Though the present work was basically done to trace the fracture path in an welded asperity junction, it can be very easily used in any problem where the path of fracture is of interest. As an example a notched plate subjected to

uniform tensile loading on one edge and fixed along the other edge has been analysed to show the path of failure, similarly any type of structural problem can be solved using the computer code developed. Due to the versatality of the finite element technique a welded asperity junction of two different materials can also be solved with a few minor changes in the code.

The main scope of this work would be the application to estimate crater wear in cutting tools during machining, where the crater wear occurs due to basic adhesive wear. Wear studies on bearings can also fall in this category.

The original idea was to do extensive analysis of asperity failure of bimetallic junctions. Due to several limitations the work was confined to the following:

(a) Testing of FEM Model for a brittle material junction using the elastic analysis of finite elements.

(b) Analysis of fracture at the interface of a ductile junction using the elasto-plastic analysis:

  (i) when fracture occurs at the interface in only one asperity

  (ii) when fracture occurs at the interface in both the asperities forming the junction.

Chapter 2 contains a brief description of the finite element method. A non-linear FE technique using initial stress method is also described.

Chapter 3 describes the problem formulation and how exactly the crack path is traced making using of the finite element method.

In Chapter 4, the paths obtained using the FE analysis are given along with a brief note justifying the acceptability of the model proposed.

CHAPTER 2

FINITE ELEMENT APPROACH

2.1 Introduction:

The FEM's usefulness and its versatality lies in its ability to easily accommodate material nonlinearities, geometric nonlinearities and to account for complex boundary conditions. This chapter briefly outlines the theory of finite element method and its formulation. Displacement formulation of the element suitable for the analysis of crack propagation in a welded asperity junction is described using a 6-node isoparametric element. The initial stress method to solve the elasto-plastic problem is presented together with a brief discussion of the yield criteria. At the end, a brief note on the convergence of the Finite Element Method is given.

2.2 The Finite Element Method:

Since FEM is a powerful technique it was considered that it could be applied to fracture of asperity junction. The possible advantage could be that FEM can easily account for material nonlinearity, different geometries of the asperity junction and complex boundary conditions. In recent years, it has been applied extensively in many areas such as structural mechanics, soil mechanics, heat conduction etc. In

many situations an adequate engineering model of the system is obtained by replacing the system by a finite number of well defined components called as elements. Such problems are called discrete problems. Even if the number of elements is very large, the discrete problem can nowbe solved readily with the advent of digital computers. The various discretization methods suggested from time to time to solve the realistic continuum problem, both by Engineers and Mathematicians, all involve approximations which approach the true continuum solution as the number of discrete variables increase.

For problems involving complex material properties and boundary conditions the engineer resorts to numerical methods that provide an approximate but acceptable solution. In most numerical methods the solutions yields approximate values of the unknown quantities only at a discrete number of points in the body. This process of selecting only a certain number of discrete points in the body is termed as discretization.

Finite Element Method is now very well described in a number of books [24,26] . FEM is a numerical discretization procedure by the use of which a wide range of complex boundary value problems can be analysed. Elastic, non-linear elastic and elasto-plastic constitutive relations can be implemented within the finite element framework in a straightforward manner.

In FEM, the region of interest is divided into a finite number of simply connected sub-domains or elements. An approximate functional value of the solution is assumed over the sub-domain so that the parameters, say u_i ($i = 1,...n$) of the function becomes the unknown of the problem. The elements are assumed to be interconnected at discrete number of points situated on the boundaries and these points are known as nodes. The nodal displacements will be the basic unknowns. A set of functions is chosen to define uniquely the state of displacement within each element in terms of nodal displacements. The displacement functions now define uniquely the state of displacement within each finite element in terms of nodal displacements. Strains along with the constitutive properties of the material will define the state of stress throughout the element and hence along the boundaries. This is discussed in more detail in Section 2.5.

FEM is endowed with two basic features which account for its superiority over other numerical methods. First, a geometrically complex domain of the problem is represented as a collection of geometrically simple subdomains called finite elements. Second, over each finite element the approximation functions are derived using the basic idea that any continuous function can be represented by a linear combination of algebraic polynomials. The approximation functions are derived using concepts from interpolation theory and are therefore called interpolation functions. Thus the FEM can be

interpreted as a piecewise application of the variational methods, in which the approximation functions are algebraic polynomials and the undetermined parameters represent the values of the solution at a finite number of preselected points called nodes; on the boundary and in the interior of the element.

2.3 Basic Approach of FEM:

The basic concept is derived from structural analysis. Here every structure is approximated as a physical assemblage of individual structural components or finite elements. The elements are interconnected at a finite number of nodes and sometimes along the boundaries of the element. Assuming the approximate behaviour of individual elements, the behaviour of the entire system can be analysed. After assembling the individual elements, the necessary boundary conditions are imposed, with primary nodal values as unknowns. Solution of the resulting set of equations yield the system response.

Considering the nature of each individual component in an element, the relationship between the primary variable u^e and the forcing function Q^e, for a linear system can be written as [24]

$$Q_i^e = K_{ij}^e \; u_j^e \qquad (2.1)$$

repetitive indices indicating summation.

The connection among elements can be established using,

(a) One set of variables, u_j, for the assembled system, i.e. the condition of continuity

$$u_j = u_j^e$$

(b) The equilibrium of the second set of variable Q_i^e, at each node and equating it to zero,

$$\sum_{e=1}^{NEL} Q_i^e = 0 \qquad (2.2)$$

in which, NEL, is the number of elements considered using the above three equations the resulting equation can be written as

$$[K]\{u\} = \{Q\} \qquad (2.3)$$

in which

$$[K] = K_{ij} = \sum_{e=1}^{NEL} K_{ij}^e \qquad (2.4)$$

and

$$\{Q\} = Q_{oi} = \sum_{e=1}^{NEL} Q_{oi}^e \qquad (2.5)$$

2.4 Finite Element Displacement Formulation of an Elastic Continuum:

The special features are as given below [25].

The continuum is divided by imaginary lines into a finite number of elements; these elements are assumed to be

interconnected at discrete number of nodal points along their boundaries. The nodal displacements form the basic unknowns. A set of functions are chosen to define uniquely the state of displacement within each element. The displacements now define uniquely the state of strain within each element, strains together with the material properties define the state of stress within the element and along the boundary of the element.

Once this stage is reached, the solution procedure follows the standard discrete system pattern. The above procedure involves a series of approximations. Ensuring displacement compatibility between adjacent elements may not be possible always, though within each element it is obviously satisfied. Concentrating the equivalent forces at nodes, equilibrium conditions are satisfied in the overall sense only.

The displacements can be expressed as

$$U = \Sigma N_i a_i^e = [N_i, N_j, \ldots\ldots] \begin{Bmatrix} a_i \\ a_j \\ \vdots \end{Bmatrix}^e = Na^e \qquad (2.6)$$

where U = displacement at any point within the element

N = prescribed function of position called shape function

a^e = nodal displacement vector for a particular element.

The strain vector, ε, can be obtained with displacements known at all points within the element,

$$\{\varepsilon\} = [B]\{a\} \tag{2.7}$$

For a linearly elastic constitutive law,

$$\{\sigma\} = [D]\{(\varepsilon - \varepsilon_o)\} + \{\sigma_o\} \tag{2.8}$$

where,

$\{\varepsilon_o\}$ = initial strain matrix

$[D]$ = stress strain matrix

$\{\sigma_o\}$ = initial residual stresses

$q^e = \begin{Bmatrix} q_i^e \\ q_j^e \\ \vdots \end{Bmatrix}$ = nodal force vector which are statically equivalent to the boundary stresses and distributed loads on the elements.

2.5 Displacement Formulation of the Element Used:

The unique description of the displacement within each element in terms of nodal values at boundary points or internal points of the element is the basic step in any displacement finite element formulation and can be expressed as

$$\{U\} = [N]\{a^e\} \tag{2.9}$$

where $[N]$ is the matrix of shape functions.

If the shape function chosen to describe the element geometry are identical to those used to prescribe function (displacement) variation, then the element is termed isoparametric. The basic procedure in the isoparametric formulation is to express the element coordinates and element displacements in the form of interpolation functions using natural coordinate system of the element. The functional property of the interpolation function N_i is that its value in the natural coordinate system is unity at node i and zero at all the other nodes. The formulation given below follows the general pattern of derivation suggested by Bathe and Wilson [26] and Zienkiewicz [24]. For a 2-dimensional triangular element, interpolation functions for a 6-noded case is given below. N_i can be derived from the general quadratic relationship

$$N_i = a_1^{(i)} L_1 + a_2^{(i)} L_2 + a_3^{(i)} L_3 + a_4^{(i)} L_1L_2 + a_5^{(i)} L_2L_3 + a_6^{(i)} L_1L_3 \qquad (2.10)$$

(REFER APPENDIX A.1)

A quadratic variation of displacement and geometry are assumed for this element and it has 12-displacement degrees of freedom (Fig. 2.1).

Similarly, the displacements expressed in terms of nodal values are:

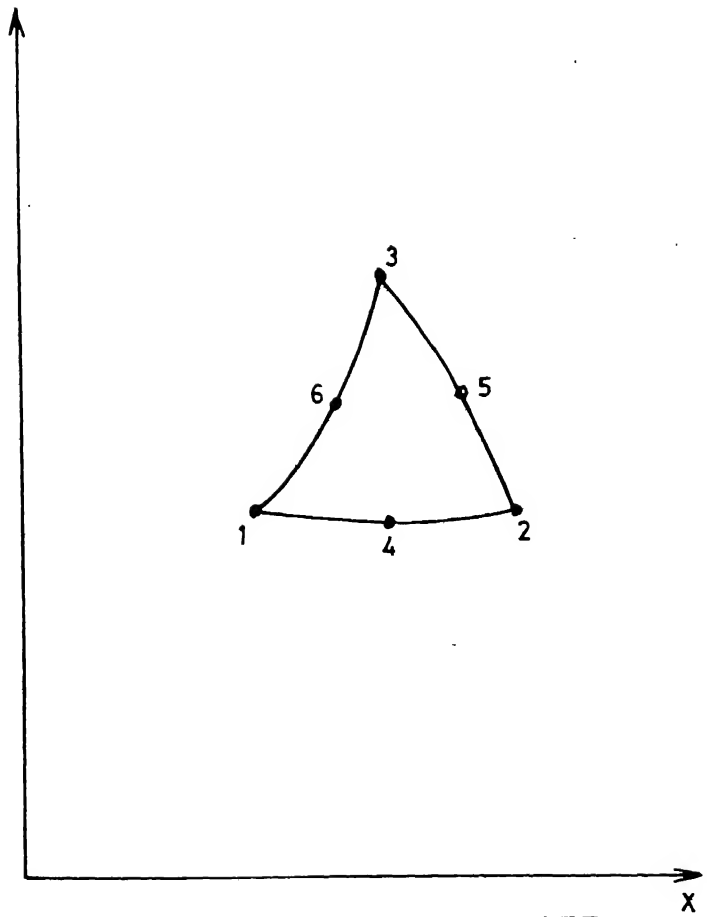

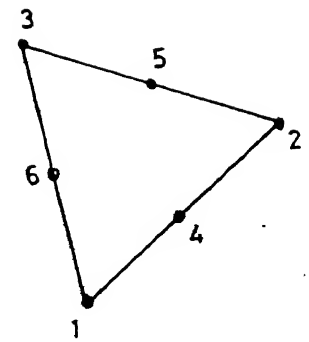

IN NATURAL COORDINATES

FINITE ELEMENT USED

FIG. 2.1

$$U = N_1u_1 + N_2u_2 + N_3u_3 + N_4u_4 + N_5u_5 + N_6u_6 \quad (2.11)$$

$$V = N_1v_1 + N_2v_2 + N_3v_3 + N_4v_4 + N_5v_5 + N_6v_6 \quad (2.12)$$

along the edge of theelement the variation of displacement is quadratic.

Writing equations 2.11 and 2.12 in matrix notation

$$\{u\} = [N]\{a\} \quad (2.13)$$

where

$$\{a\}^T = [u_1\ v_1\ \ u_2v_2\ \ u_3v_3\ \ u_4v_4\ \ u_5v_5\ \ u_6v_6] .$$

The strains at any point within the element is obtained knowing the nodal displacement, by,

$$\{\varepsilon\} = [B]\{a\} \quad (2.14)$$

where $[B]$ is the strain displacement matrix (REFER APPENDIX A.2).

The stress at any point within the element is now obtained knowing the strain vector and the stress strain matrix $[D]$ by

$$\{\sigma\} = [D]\{\varepsilon\} \quad (2.15)$$

where [D] is the stress-strain matrix for plane stress (REFER APPENDIX A.3).

The matrix to be evaluated are the stiffness matrix $[K_e]$. $[K]$ is evaluated by numerical integration of

$$t \int_{A(e)} B^T D\ B\ dA \quad (2.16)$$

$$[K_e] = |J| t \sum_{i=1}^{n} w_i f(L_1^{(i)}, L_2^{(i)}, L_3^{(i)}) \qquad (2.17)$$

n stands for the number of Gauss point, J is the Jacobian matrix,

$$[J] = \begin{bmatrix} \partial x/\partial L_1 & \partial y/\partial L_1 \\ \partial x/\partial L_2 & \partial y/\partial L_2 \end{bmatrix} \qquad (2.18)$$

w_i = weighting functions of gauss point where n for quadratic element is 3. Zienkiewicz [24] has given the following weighting functions for quadratic triangular element using Gaussian quadrature formula with 3 points.

2.6 Elasto-plastic Analysis:

The difference between elastic and plastic behaviour under uniaxial stress is brought out in Fig.2.2. In non-linear elastic behaviour the stress can be expressed as a function of strain as $\sigma = \sigma(\varepsilon)$. The main difference of plasticity formulation from nonlinear elastic formulation is such an explicit relationship is not available. Although the stresses at any level of strain have to lie on or within the current yield surface, the exact value of each component cannot be determined.

Many numerical solutions of elasto-plastic problems by FEM have been developed, the most common are as listed below:

(1) Incremental tangential stiffness approach;

(2) Initial strain method; and

(3) Initial stress method [27].

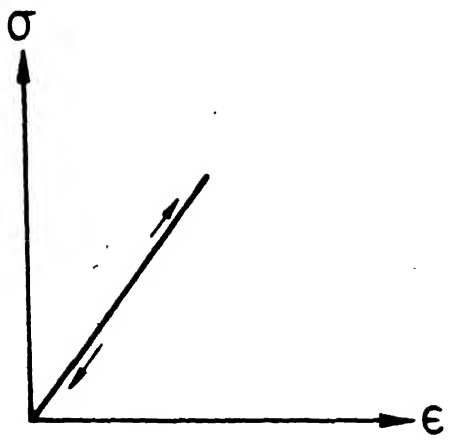

a. Linear elastic

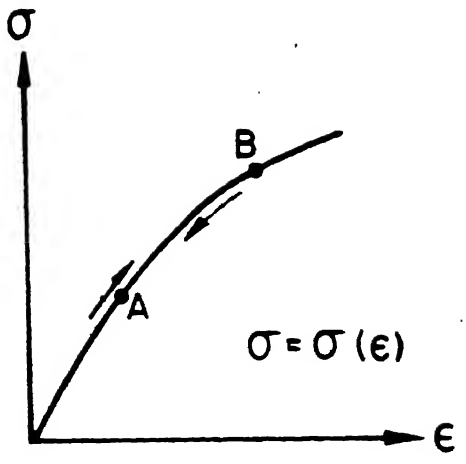

b. Non-linear elastic

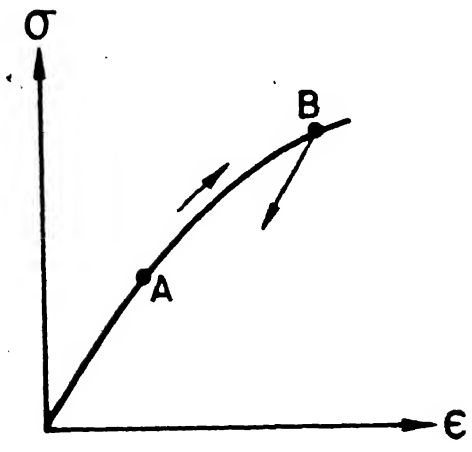

c. Strain hardening plasticity

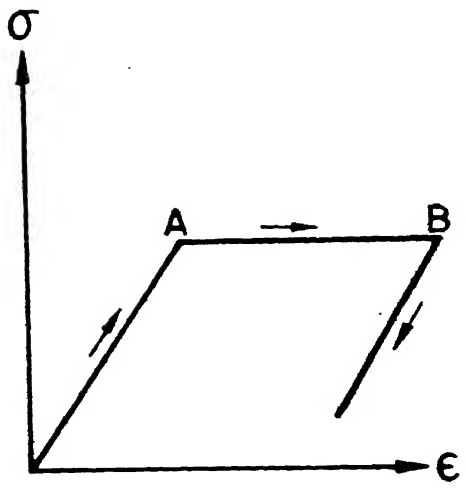

d. Ideal plasticity

Fig. 2.2 Elastic and plastic behaviour under uniaxial stress

Initial strain method fails to converge for perfect plasticity and a small degree of work hardening because of the large plastic strains that occur. Initial stress method overcomes this difficulty because it relies on the fact that a unique stress exists for a increment of strain. Hence the last one is more popular and is discussed in detail in this chapter.

2.7 Yield Criteria:

A yield criteria is a hypothesis concerning the limit of elasticity under any possible combination of stresses. The suitability of any proposed yield criteria must be checked by conducting experiments. It has been shown that the yield criteria is a function of $(\sigma_1 - \sigma_2)$, $(\sigma_2 - \sigma_3)$ and $(\sigma_3 - \sigma_1)$ and is independent of the hydrostatic stress component $(\sigma_1 + \sigma_2 + \sigma_3)/3$.

Thus yielding occurs when some scalar function of the principal stress differences reaches a critical magnitude, mathematically:

$$f(\sigma_1 - \sigma_2, \sigma_2 - \sigma_3, \sigma_3 - \sigma_1) = \text{constant} \quad (2.19)$$

The two of the most commonly used yield criterias are:

(1) Tresca Yield Criteria

(2) Von-Mises Yield Criteria.

Von-Mises yield criteria used in this work is discussed below:

Von-Mises Yield Criteria:

Mathematically it can be stated as,

$$(\sigma_1 - \sigma_2)^2 + (\sigma_2 - \sigma_3)^2 + (\sigma_3 - \sigma_1)^2 = \text{constant} \qquad (2.20)$$

In this function, each of the principal stresses contribute to yielding. The criteria was interpreted by Hencky as "Yielding begins when the shear strain energy reached a critical value".

The value of the constant in the above criteria can be determined from the simple tension yielding, i.e. $\sigma_1 = \sigma_{yp}$, $\sigma_2 = 0$, $\sigma_3 = 0$ and pure shear yielding, i.e. $\sigma_1 = -\sigma_3 = K$, $\sigma_2 = 0$. Hence the Yield Criteria becomes,

$$(\sigma_1 - \sigma_2)^2 + (\sigma_2 - \sigma_3)^2 + (\sigma_3 - \sigma_1)^2 = 2\sigma_{yp}^2 = 6K^2 \qquad (2.21)$$

where σ_{yp} = tensile yield stress and K is yield shear stress.

For a general state of stress (σ_x, σ_y, σ_z, σ_{xy}, σ_{yz}, σ_{zx}). The Von-Mises yield criteria can be expressed as

$$\frac{1}{\sqrt{2}}\left[(\sigma_x - \sigma_y)^2 + (\sigma_y - \sigma_z)^2 + (\sigma_z - \sigma_x)^2 + 6(\tau_{xy}^2 + \tau_{yz}^2 + \tau_{zx}^2)\right]^{1/2} = \sigma_{yp} \qquad (2.22)$$

Figure 2.3 shows both the yield criteria represented in principal stress space and π plane, respectively.

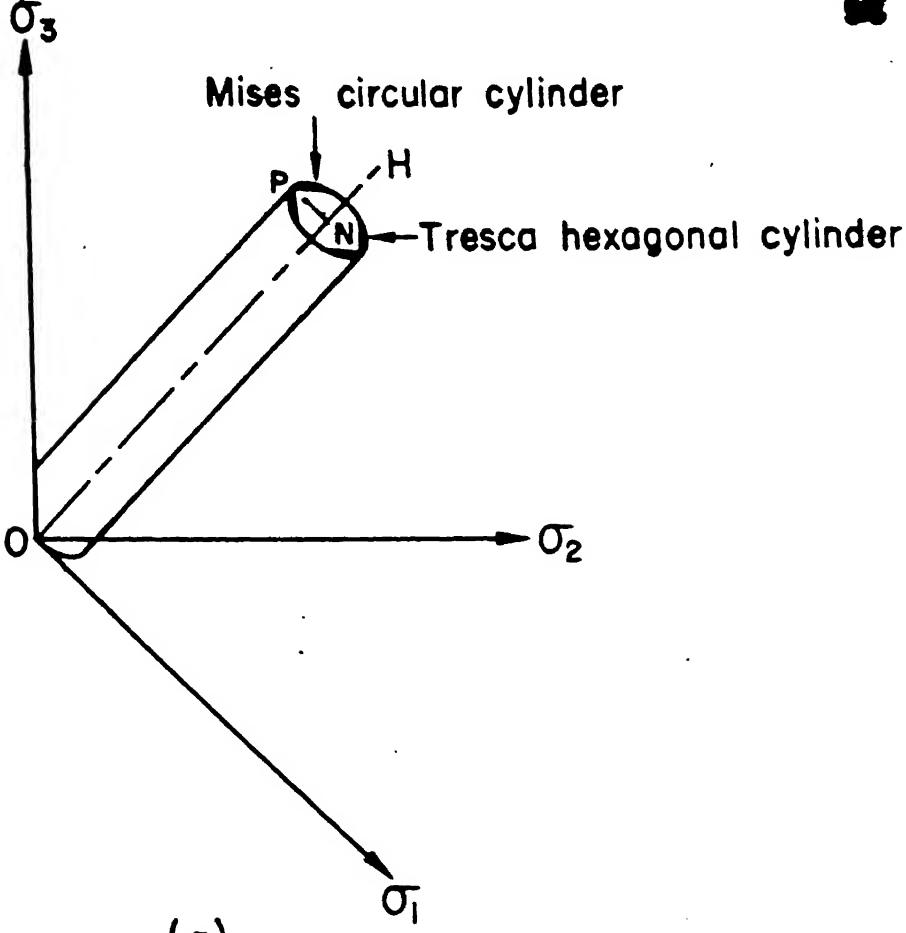

(a)

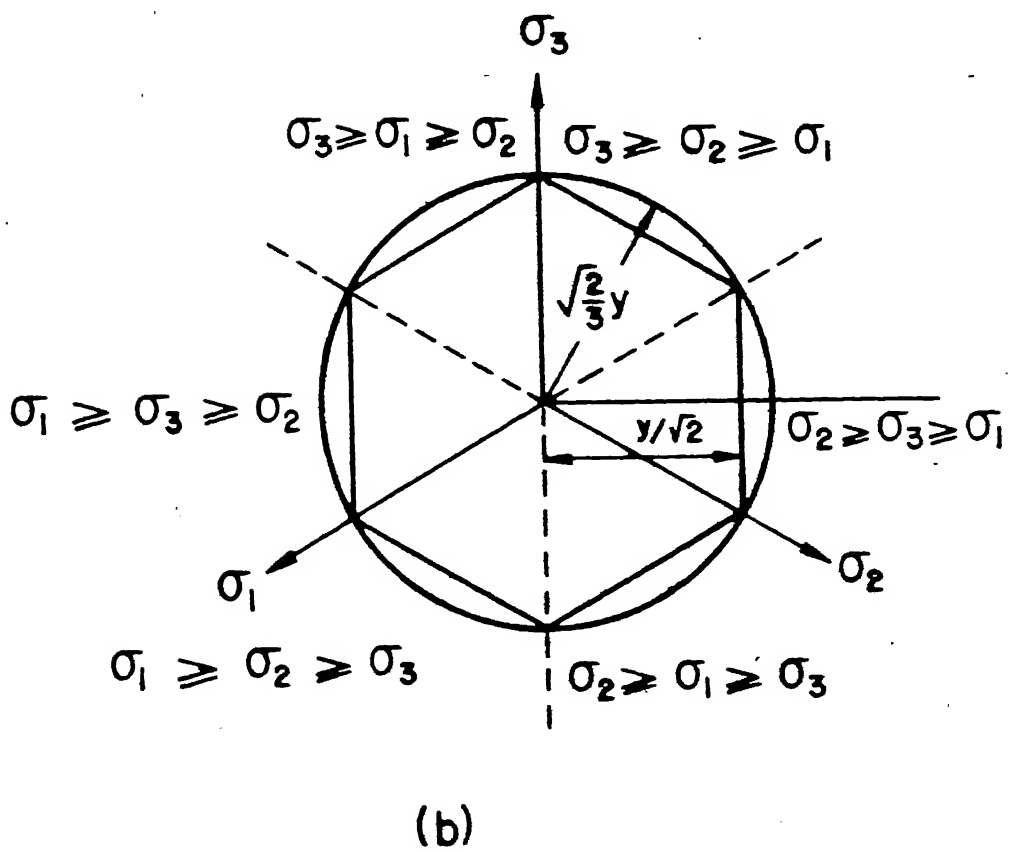

(b)

Fig. 2.3 Stress space representation of yield criteria.

2.8 Elasto-plastic Stress-strain Matrix:

Hookes Law for the isotropic elastic material can be written in the matrix form as $\{\sigma\} = [D]\{\varepsilon\}$.

Yamada and Yoshimura [28] have developed a plastic stress-strain matrix $[D_p]$ (SEE APPENDIX A.4) by inverting the Prandtl-Reuss equations obeying the Von-Mises yield criterion.

For the plane stress case the $[D_p]$ matrix will reduce to the following as given by Yamada and Yoshmura [28]

$$D_p = \frac{E}{Q}\begin{bmatrix} \sigma_y'^2 + 2p & & \\ (-\sigma_x'\sigma_y' + 2\nu p) & (\sigma_x'^2 + 2p) & \text{Symmetric} \\ \left(-\frac{\sigma_x' + \nu\sigma_y'}{1+\nu}\tau_{xy}\right) & \frac{(-\sigma_y' + \nu\sigma_x')}{1+\nu}\tau_{xy} & \frac{R}{2(1+\nu)} + \frac{2H'}{9E}(1-\nu)\bar{\sigma}^2 \end{bmatrix}$$

where,

$$p = \frac{2H'}{9E}\bar{\sigma}^2 + \frac{\tau_{xy}^2}{1+\nu} \qquad (2.23)$$

$$Q = R + 2(1-\nu^2)p \qquad (2.24)$$

$$R = \sigma_x'^2 + 2\nu\sigma_x'\sigma_y' + \sigma_y'^2 \qquad (2.25)$$

σ_x' and σ_y' stand for the deviatoric stresses.

The elasto-plastic matrix is then given by

$$[D_{EP}] = [D] - [D_p] \qquad (2.26)$$

2.9 The Initial Stress Computational Method:

In the initial stress method [27] the solution of the non-linear problem is approached in a series of approximations. During a load/displacement increment, a purely elastic problem is solved, determining an increment of strain $\{\Delta\varepsilon'\}$ and stress $\{\Delta\sigma'\}$ at every point in the continuum. For the increment of strain found from the analysis, the stress increment in general will not be correct. If $\{\Delta\sigma\}$ is the true increment of stress possible for the given strain then the situation can only be maintained by a set of body forces, equilibrating the initial stress system given by $\{\Delta\sigma'\} - \{\Delta\sigma\}$. At the second stage of the computation, this body force system can be removed by allowing the structure (with unchanged elastic properties), to deform further. An additional set of strain and corresponding stress increments are caused. Once again these are likely to exceed those permissible by the non-linear relationship and the redistribution of equilibrating body forces has to be repeated. If the process converges then within an increment the full non-linear, compatibility and equilibrium, conditions will be satisfied. In each cycle, since the same elastic problem is solved only partial inversion of the elastic equations is needed.

For the elastic-plastic situation, the steps during a typical load/displacement increment can be summarised as follows [27]:

1. Increment of load/displacement is applied. Elastic increments of strains $\{\Delta\varepsilon'\}_1$ and corresponding elastic increments of stress $\{\Delta\sigma'\}_1$ are determined.

2. $\{\Delta\sigma'\}_1$ is added to stresses existing at start of increment, $\{\sigma_o\}$, to obtain $\{\sigma'\}$, and thus $\bar{\sigma}'$. Check whether $\bar{\sigma}' < \sigma_{yp}$. If the condition is satisfied only elastic strain changes occur and the process is stopped. If the condition is not satisfied proceed to the next step.

3. If $\bar{\sigma}' \geq \sigma_{yp}$ and if $\bar{\sigma}'_o = \sigma_{yp}$ (the element has yielded at the start of iteration), $\{\Delta\sigma\}_1$ is found by
$$\{\Delta\sigma\}_1 = [D_{EP}]\{\Delta\varepsilon'\}_1 \qquad (2.27)$$
where D_{EP} is computed using $\{\sigma'\}$. Stresses which are supported by body forces are evaluated
$$\{\Delta\sigma''\}_1 = \{\Delta\sigma'\}_1 - \{\Delta\sigma\}_1 \qquad (2.28)$$
Current stress is
$$\{\sigma\} = \{\sigma'\} - \{\Delta\sigma''\}_1 \qquad (2.29)$$
Current strain is
$$\{\varepsilon\} = \{\varepsilon'\} + \{\Delta\varepsilon\}_1 \qquad (2.30)$$

4. If $\bar{\sigma}' > \sigma_{yp}$, but $\bar{\sigma}'_o < \sigma_{yp}$, i.e., elastic-plastic transition has occurred in that iteration, a factor H from equation (2.31) is found and then the intermediate stress value is found out at which

yielding begins. The increment in stress is computed by the relation, $\{\Delta\sigma_1\} = [D_{EP}]\{\Delta\varepsilon'\}_1$ starting from that point. Then proceed as in step 3 with $[D_{EP}]$ computed from stresses $\{\sigma'\}$.

$$\text{Factor} = \frac{\bar{\sigma}' - \sigma_{yp}}{\bar{\sigma}' - \bar{\sigma}_o} \qquad (2.31)$$

5. Nodal forces are computed corresponding to the equilibrating body forces. These are given by

$$\{R_L\}^e_1 = \int [B^T]\{\Delta\sigma''\}_1 \, d(\text{vol}) \qquad (2.32)$$

elemental nodal force are added to get the complete nodal force vector $\{R_L\}$.

6. The problem is resolved using the original elastic properties and the load system $\{R_L\}$ to find $\{\Delta\sigma'\}_2$ and $\{\Delta\varepsilon'\}_2$.

7. Current values are found.

8. Steps 2 to 6 are repeated.

The cycling can be stopped when the appropriate convergence criterion specified is satisfied.

2.10 Convergence of the Iterative Procedure:

The adoption of an incremental plasticity theory and iterative solution technique, such as used in "Initial Stress Method" leads to errors due to size of increment and finite values of criteria specified in a solution, indicate whether the non-linear equations describing the behaviour of

the material when subjected to increments of load/displacement have been solved with sufficient accuracy. This is achieved by comparing the change in some aspect of the solution between iterations and terminating the procedure once this change has become sufficiently small.

Nayak and Zienkiewicz [29] have described some of the convergence criteria for load based analysis and displacement based analysis. The convergence criteria imposed in this work is on the change in the absolute magnitude of largest term in load correction vector between the iterations, compared as a percentage of the absolute magnitude of largest term in load correction vector at that instant calculated by equation (2.33),

$$C = \frac{R_{L_{max\ i}} - R_{L_{max\ i+1}}}{R_{L_{max\ i+1}}} \qquad (2.33)$$

where,

C = convergence criterion

$R_{L_{max\ i}}$ = magnitude of largest term in residual load vector at ith iteration

$R_{L_{max\ i+1}}$ = magnitude of largest term in residual load vector at $(i+1)^{th}$ iteration.

The following chapter briefly outlines the problem formulation and how the path of crack is determined using FEM. A note on formation of double nodes as crack propagates is also given.

CHAPTER 3

PROBLEM FORMULATION AND METHODOLOGY

3.1 Introduction:

This chapter describes the details of the actual problem of welded asperity junction and the finite element methodology of tracing the path of crack in the asperity junction. The asperity junction fracturing is considered as occurring under plane stress conditions. Six-node isoparametric triangular elements are used for the analysis and numerical integration is employed for calculating stresses and strains. A list of the assumptions and the description of the data which is necessary for the execution of the programme is also mentioned, together with the solution procedure. The criteria used to determine crack initiation and propagation is also stated.

3.2 Problem Description:

The asperity junction is considered at a stage of its life cycle wherein it is symmetrical as shown in Fig. 3.1 . For the present analysis, the function as it fractures is simplified as occurring under plane stress conditions. In this work an attempt has been made to obtain the distribution of stress and strain at the nodes which is then used to trace

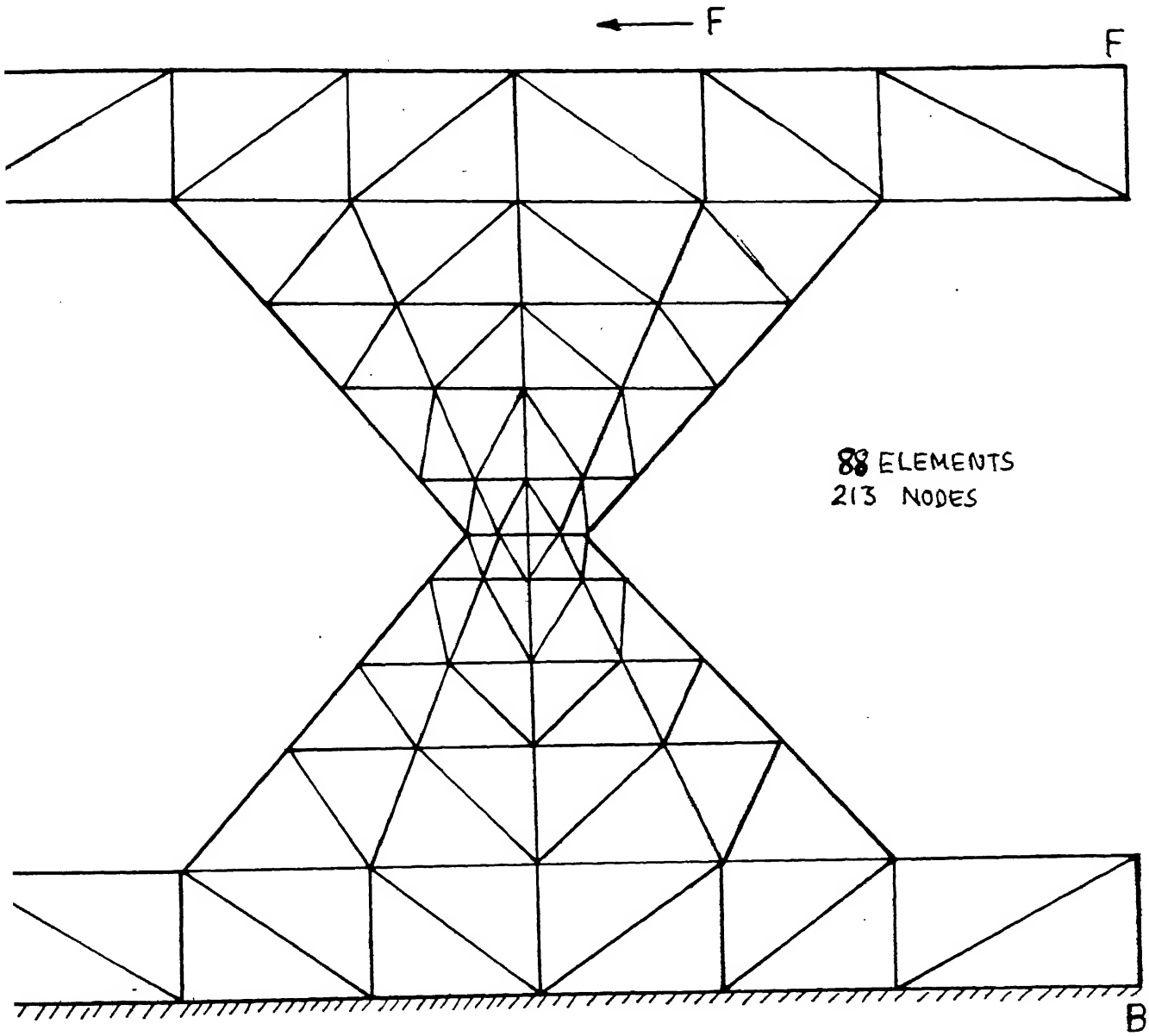

FIG.3(b) FINITE ELEMENT MESH USED

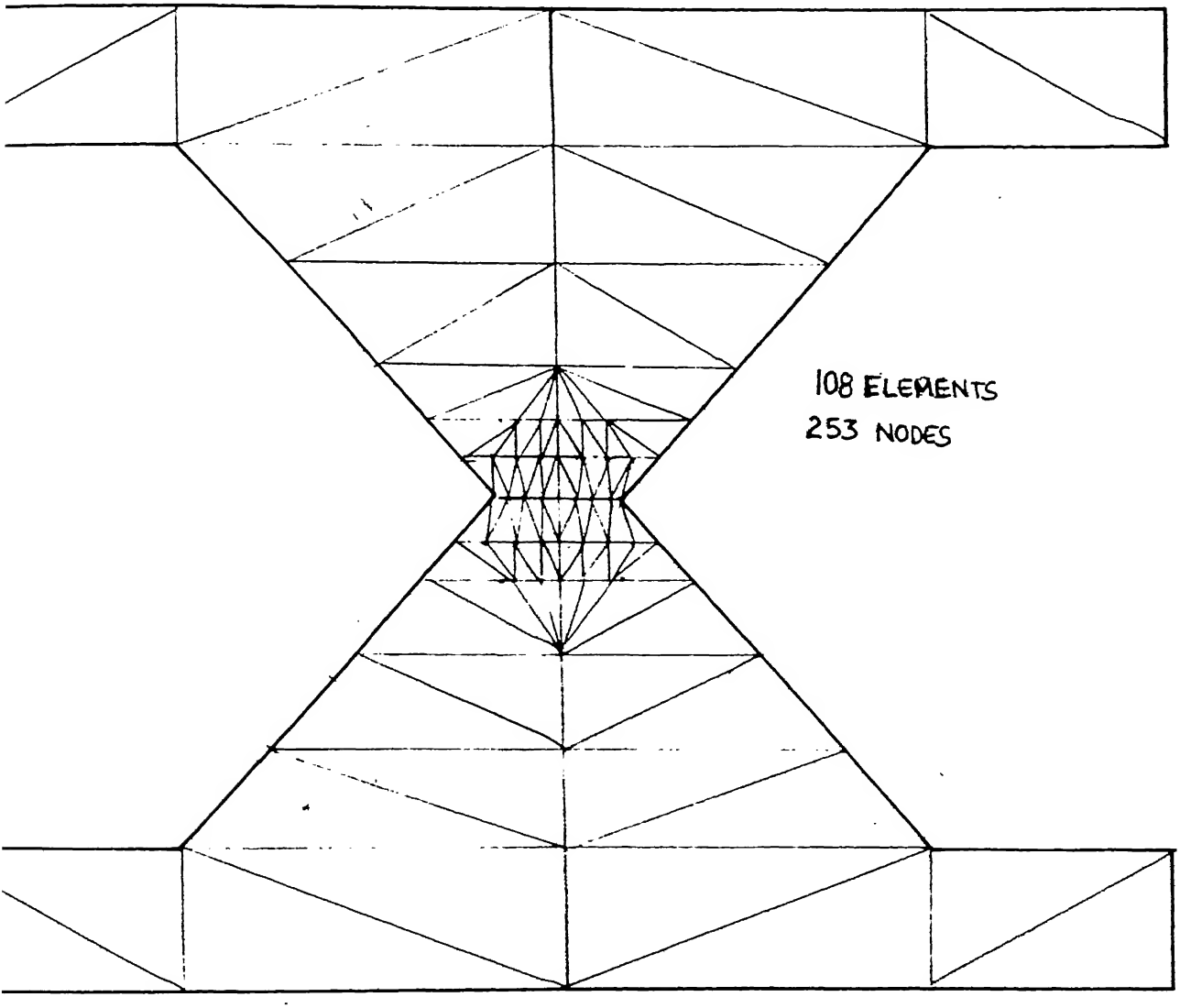

FIG 3.4(b) FINEST FEM MESH USED

the path of crack.

The process of junction fracture is analysed using the finite element method with the following assumptions:

(i) The junction geometry is assumed to be perfectly symmetrical about the interface.

(ii) The junction failure is assumed to occur under conditions of plane stress.

(iii) Small deformation theory is applicable for the purpose of calculating stresses and strains.

(iv) For the ductile junction considered the material considered is isotropic, linearly elastic, linear strain hardening type obeying the Von-Mises yield criterion.

The following geometric boundary conditions and force conditions are specified for the present work as shown in Fig. 3.1 :

(i) The boundary AB is fixed both in the X and Y directions.

(ii) The boundary EF is subjected to force boundary conditions in the X direction.

3.3 FE Formulation and Crack Propagation:

The problem described above is solved using FEM explained in Chapter 2. The asperity junction is discretized as shown in Fig.3.1. The study of wear, involved the modelling of crack propagation usually emanating from the asperity junction.

The propagation is simulated by using the concept of double nodes.

The crack propagation in finite element method is simulated by making each node along the crack path into two nodes (double nodes) once the crack passes through that node. Consider a path along which crack is going to propagate as shown in Fig.3.2. As the crack passes through the node i, it has to be replaced by two nodes and as the crack passes through the node j another two nodes have to replace the node j, because the elements I and II are now no longer connected at i & j as was the case before the crack propagated along that edge. Due to this formation of double nodes the node numbering has to be redone and a brief description on how it is done is given below.

The elements connected to node i (before crack propagates) are all identified and the slopes made by node i joining their (elements) midnodes on edge opposite to i are found out and stored. Now the angle made by the crack along the edge of element to reach the node is found out, say θ_1, this angle is with reference to node i. The path along which crack now is going to pass is identified and the angle made by that path with respect to node i is again identified, say θ_2. At this stage the node number of i and j are compared as to find out which one is greater. With this information the node renumbering can be done as follows:

if i > j, then

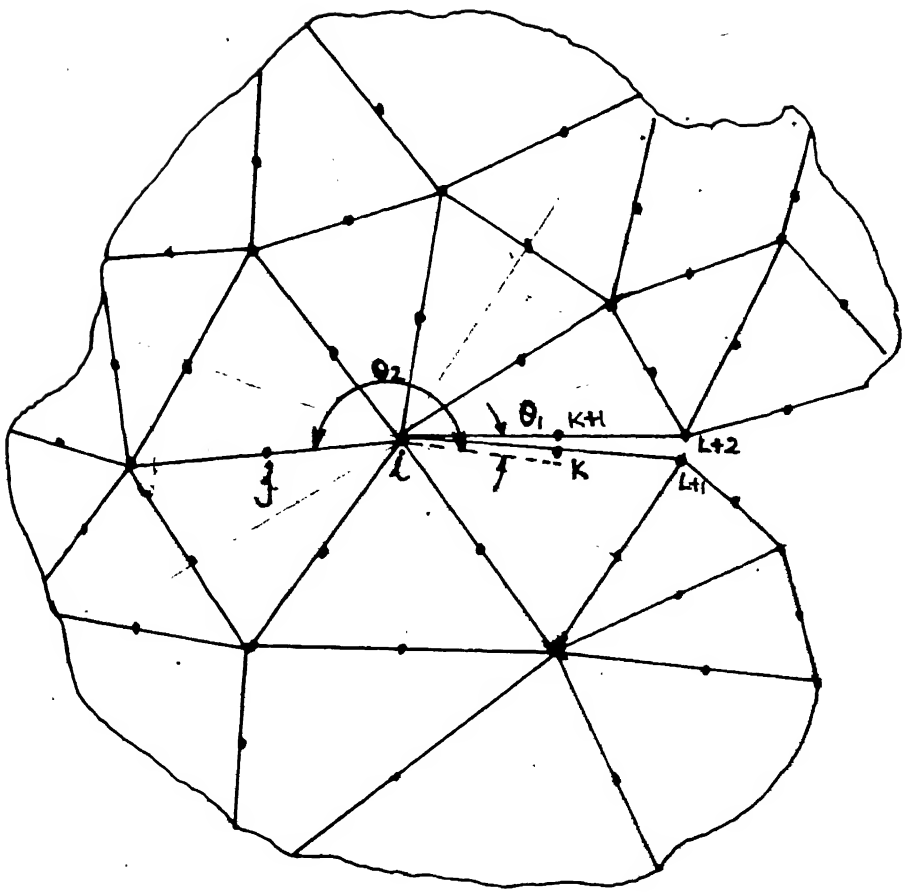

FIG 3.2 FORMATION OF DOUBLE NODES

(i) for all elements connected to node i and slope made by mid point with i; between θ_1 and θ_2 increase i to i+1.

(ii) for all elements connected to node i and slope made by mid point with i; not between θ_1 and θ_2 increase i to i+2.

(iii) for all elements having node numbers greater than i increase node number by 2.

(iv) for all nodes having node number between i and j increase node number by 1.

(v) for element containing node j if slope made by mid point with i between θ_1 and θ_2, no change in node number j.

(vi) for element containing node j and if slope not between θ_1 and θ_2 increase node number to j+1.

(vii) for nodes having number below j no changes.

Similarly a set of rules for renumbering, if j > i .

Because of the crack the nodal numbers change and due to this a new connectivity of elements has to be generated to account for the crack using the node numbers as given by the above set of rules. However it is to be noted here that the coordinates of the double nodes are assumed to have the same coordinates as that of the parent node. Thus it is clear that though the node number and connectivities have changed the elemental stiffness matrices stored on tape are unchanged. Using these elemental matrices

and new connectivities generated the global stiffness matrix is reassembled.

Thus it is seen that crack propagation requires (i) double node formation; (ii) node renumbering and (iii) corresponding change in connectivity and (iv) reassembly of global matrix.

All this has been incorporated in the computer code developed.

3.4 Direction of Crack Propagation:

From the finite element programme the forces, displacements, stresses and strains within the junction are found out. From the experimental studies it was observed that the crack initiates at the interface, using this, (i.e. knowing the particular node at which the crack initiates) all the paths (i.e. sides of elements) along which the crack can possibly propagate are investigated to see if the criteria for crack to occur has been satisfied.

The procedure for checking the criterion is briefly outlined below. Consider a small section (Fig. 3. 3) wherein the crack has propogated till node "B". Now the possible paths for the crack to propogate are BC, BD, BE, BF, BG, BH, and the possible elements are I, II, III, IV, V, VI, VII. First of all the elements along which the crack can possibly occur are identified in the continuum, along with the identification of the elements. The possible paths and the coordinates of the

... POSSIBLE PATHS
... ELEMENT NUMBERS

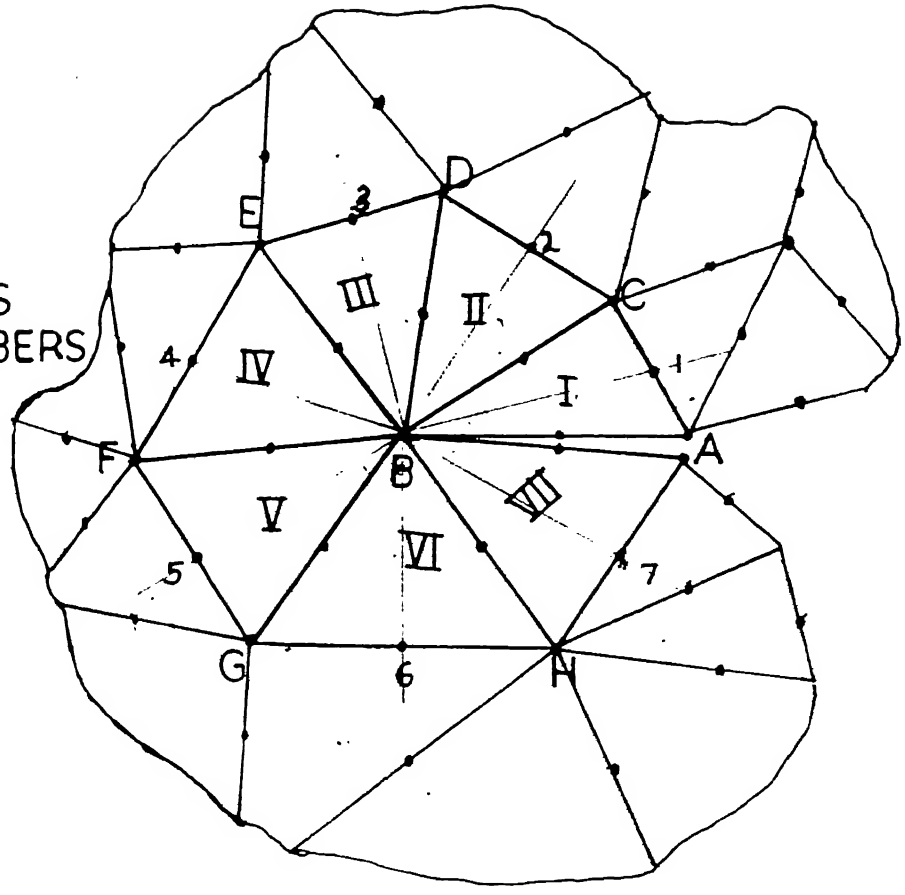

FIG. 3.3 CHECKING ALL POSSIBLE PATHS OF FRACTURE

corresponding nodes involved (i.e. end nodes of path and mid node along path) are found out. The position of the elements around the node "B" are identified by finding out the slope made by line joining "B" to mid node of the side opposite B (eg. line B1). Also, the slopes made by the possible paths are also found out and stored. Now, if the crack was to propagate along BE then the shear stress along the edge BE of Element III would have to exceed the maximum permissible shear stress of the material. To find this tangential stress, firstly the force contribution at node B from all elements lying between ABE are summed up, the component of the force along the line BE of this force is found out and this is then divided by the length of the side BE to give the tangential stress along "BE". If the crack criterion is satisfied then the crack is assumed to have proceeded along BE. Now, the node number along the path of crack are noted and using these the double nodes formed due to the crack are correctly numbered and all previous node numbers above the cracked node number also undergo changes. Because of this change in node numbers the global stiffness matrix at each stage will be different. Hence, using the stored elemental matrix we can again assemble the global stiffness matrix in accordance to the new connectivity generated within the programme. From this step the process is again repeated as above till the other edge of the junction is reached.

3.5a Methodology for Brittle Materials:

Using the FEM the stresses at all points in the continuum are got and knowing the node from which the crack will emanate all possible paths from that node are identified and checked to see if crack can propagate along it as mentioned in Section 3.4. Node renumbering etc. as mentioned in Section 3.3 due to double node formation because of crack is done. Again the whole process is repeated till the other edge of the junction is reached.

3.5b Methodology for Ductile Junction:

The procedure for the analysis of crack path is more or less similar except for the fact that here nonlinear FEM analysis using the "Initial stress" method is used. Here, the load is applied in steps, and at each step the possible crack paths are analyzed and checked if crack criteria is satisfied. If the crack has propagated the procedure as mentioned for brittle junctions, i.e. from changing nodal numbers to again checking for crack propagation is repeated. In case the crack does not propagate along any path then the next load increment is applied and so on.

In this incremental cum iterative technique of elastic-plastic finite element analysis the size of the increment and the number of iterations to be performed within an increment will affect the results obtained. For this work, the

values of load specified in the first load step is such that yielding just begins. It has been observed that by using the initial stress method for the nonlinear material problems even for large values of load/displacement increments, the results obtained are quite satisfactory. Because of the large computer storage required and large execution time of programme the number of load steps has been kept very small in the present work.

3.6 Input Data Structure:

The following data was supplied as input for the purpose of analysis:

(1) Total number of nodes and elements, weighting function for numerical integration, maximum number of iterations for each load increment, bandwidth of matrix, etc.

(2) Material properties like values of elastic modulus, Poissons ratio, yield stress, ultimate shear stress, strain hardening coefficient.

(3) Nodal data this includes the node number and the x,y coordinates of the node for all the nodes.

(4) The element data in which the element number is given and the nodal connectivities of the element, for all the elements.

(5) The boundary node number on which the boundary condition is known and the type of boundary condition on that node.

A brief description of the results obtained and the correlation with some known results are briefly described in

CHAPTER 4

RESULTS AND DISCUSSIONS

4.1 Introduction:

This chapter presents an analysis of the results obtained for the fracture path of the welded asperity junctions. The finite element analysis has been done using three type of meshes. The coarse mesh had 213 nodes with 88 elements and the fine mesh had 253 nodes with 108 elements. The CPU time required for one run of the elasto-plastic analysis on an average has been around 12-15 minutes on the DEC 1090 computer system.

The elasto-plastic computer code developed has been compared with a cantilever beam problem [27] . Load versus displacement diagram has been plotted (Fig.4.1) and the results compared fairly well with that of [27] ; Zienkiewicz [27] has used 150 triangular elements with a total of 99 nodes, whereas the present analysis used to check the computer code had 24 six-node isoparametric elements with a total of 63 nodes.

Figure 3.1 shows the finite element discretization of the asperity junction together with the geometric boundary conditions applied. The meshes have been made manually and finer meshes were not tried out, because that would have involved a higher CPU time.

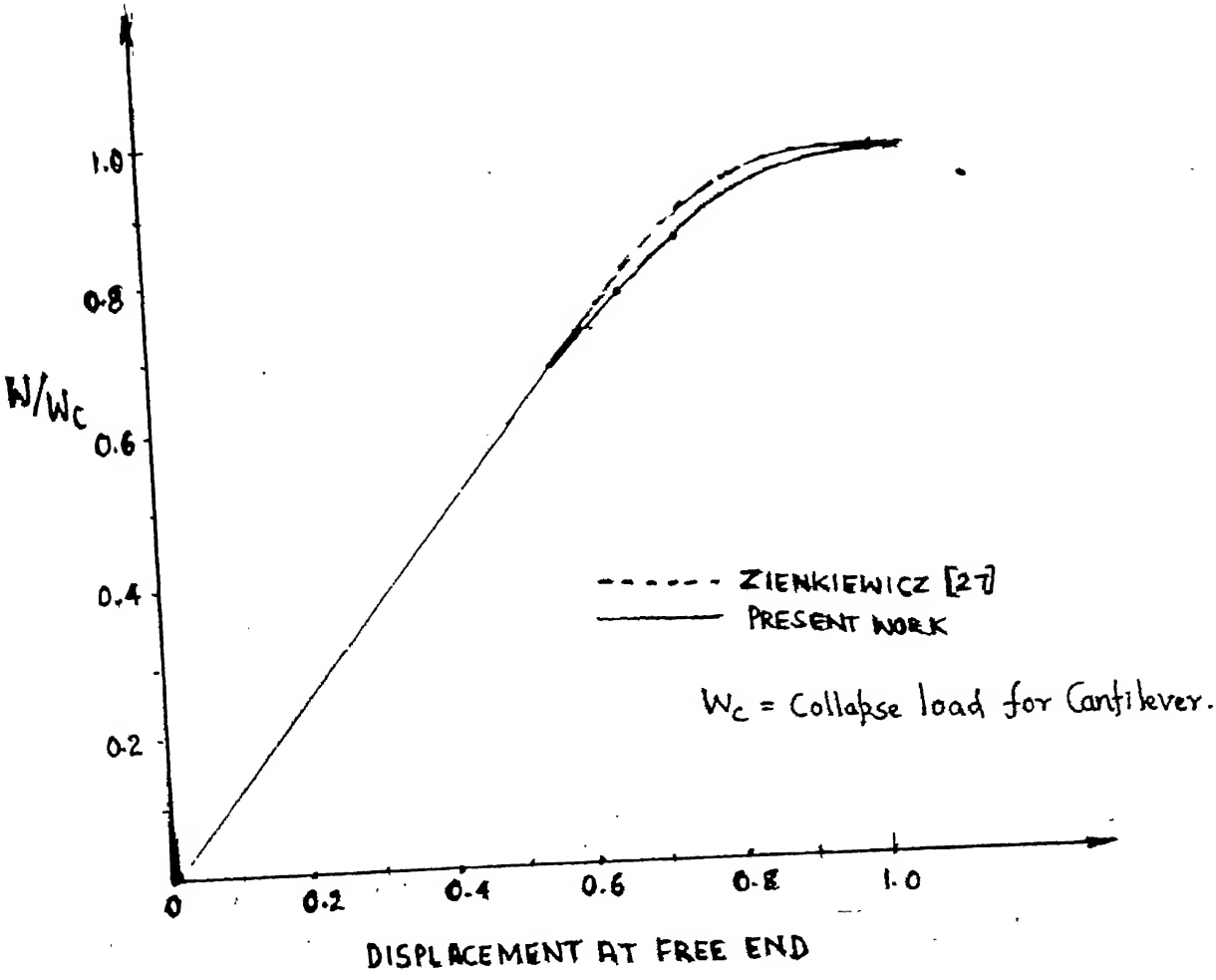

FIG 4.1 LOAD VERSUS DISPLACEMENT

4.2 Brittle Junction Failure:

In the case of asperity junctions of the two brittle materials as mentioned earlier, the elastic analysis of the continuum was done. The calculations showed that fracture started at edge A (Refer Fig. 4.2) on the interface and propagated along the path A-1, 1-2, 2-3, 3-4.....7-B. At each stage crack has been assumed to propagate which the shear stress along the edge of an element exceeds the ultimate shear strength of the material.

Thus the computer results obtained showed that the fracture path, which initiates at the junction edge A, has taken a straight path along the interface. This result is in agreement with the intuitive feeling with which the brittle junction case was used to test the FEM model.

The intuitive feeling was also supported by the observation that in case of brittle materials like cast iron rubbing against each other there is very less wear compared to the case of steel and other ductile materials which have good adhesive properties. If the fracture of welded junction in brittle materials would be occurring in a similar manner to that of ductile material the (adhesion) wear coefficient would not have been drastically lower for similar conditions. But several published results [15,30] have shown that wear of brittle materials is indeed much less.

The adhesive wear is shown to be governed by the equation

$$\frac{V}{T} = Z \frac{P}{H} \qquad (4.1)$$

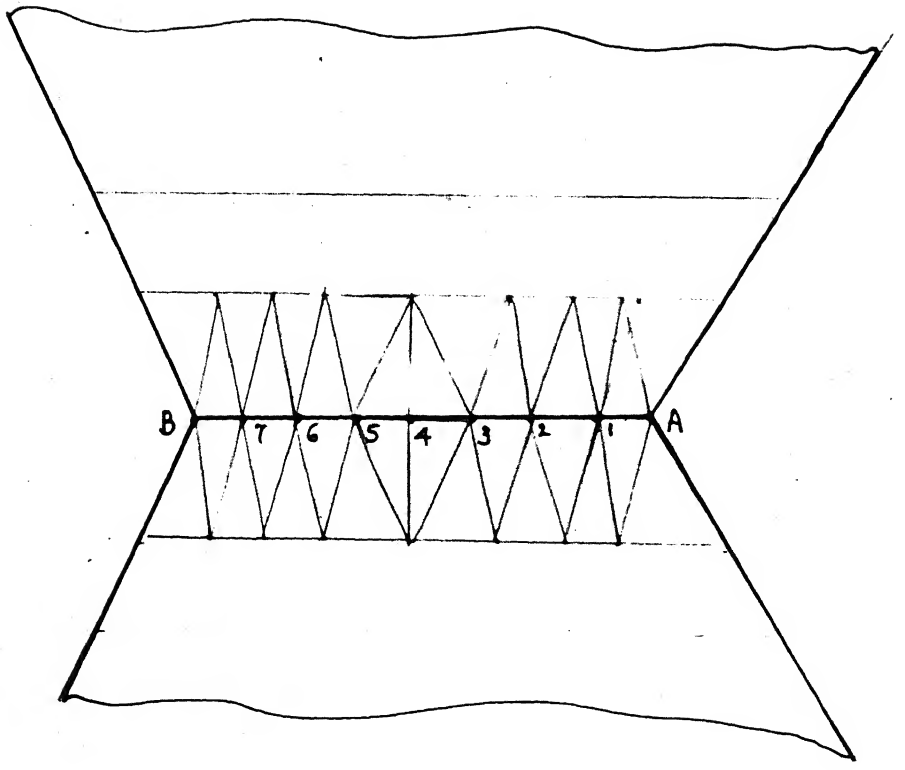

FIG.4.2 BRITTLE JUNCTION FAILURE

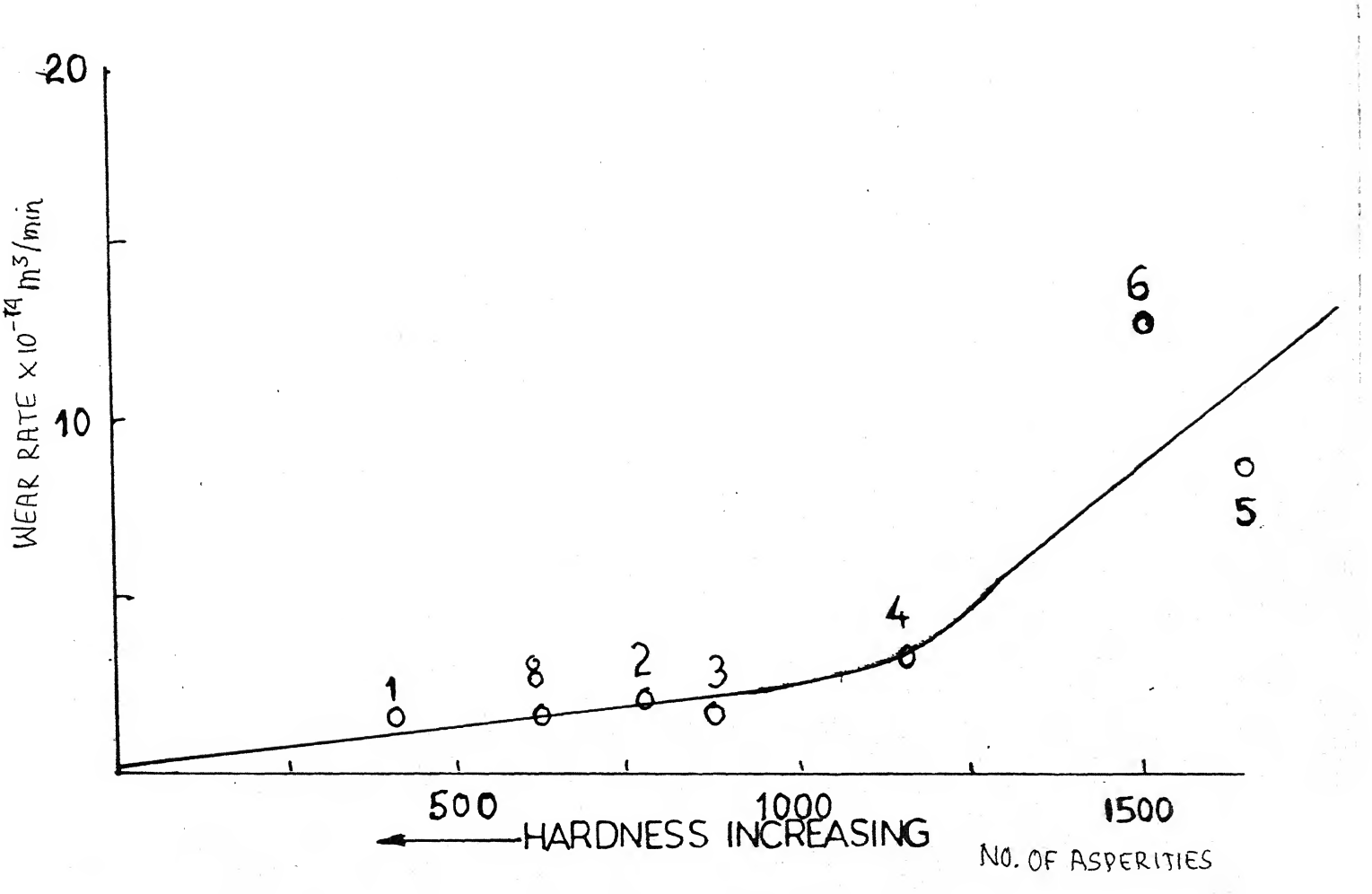

FIG.4.3 WEAR RATE VS NUMBER OF ASPERITIES (31)

where V = Volume of wear

L = Distance of sliding

Z = Wear coefficient

P = Contact load

H = Hardness of the material (softer) ;

when the two bodies are under contact the load is supported by some asperities which ultimately form junctions. The number of junctions formed can be estimated by an approximate expression [15]

$$P = HN\,a \qquad (4.2)$$

where a = Area of contact at each asperity junction supporting the load

N = Total number of asperity junctions supporting the load.

Table 4.1 shows values of Z for four different materials

TABLE 4.1 [30] :

Material	$Z \times 10^{-3}$	Remarks	Hardness
Zinc/zinc	160	High adhesion	Low
Cu/Cu	32	Medium adhesion	Medium
MS/MS	.01	Low adhesion	High
WC/WC	.001	Very low adhesion	Very high

Referring to Fig.4.3 it can be observed how the wear rate increases as the number of asperities (N) increases [31] . It can be also seen that as the hardness increases the number of asperities decrease and the wear rate also decreases. Now, since in engineering materials hardness and brittleness have a direct correlation, it is obvious that adhesion wear of hard and brittle materials is mainly by abrasion and not by adhesion. The adhesion characteristics of hard and brittle materials indeed decreases. Thus, it may not be wrong to assume that fracture in a brittle junction may be straight one as A-1.....7-B. This qualitative comparison then lends support to the inference that fracture path A-1, 1-2, 2-3, 3-4, 4-5, 5-6, 6-7, 7-B, refer Fig. 4.4 is correct and hence was considered acceptable for further application.

4.3 Ductile Junction Failure:

Trial computations were done to arrive at an approximate ultimate load for the asperity junction (P_{ap}).

For a ductile junction the elasto-plastic analysis using initial stress method was carried out and it was found that with fine mesh the fracture initiated at a load of 0.6 P_{ap}. At 0.6 P_{ap} the crack propagated from A to 1 as shown in Fig. 4.4. After making the necessary changes due to double node formation it was found that the crack did not propagate and hence another load increment of 0.1 P_{ap}

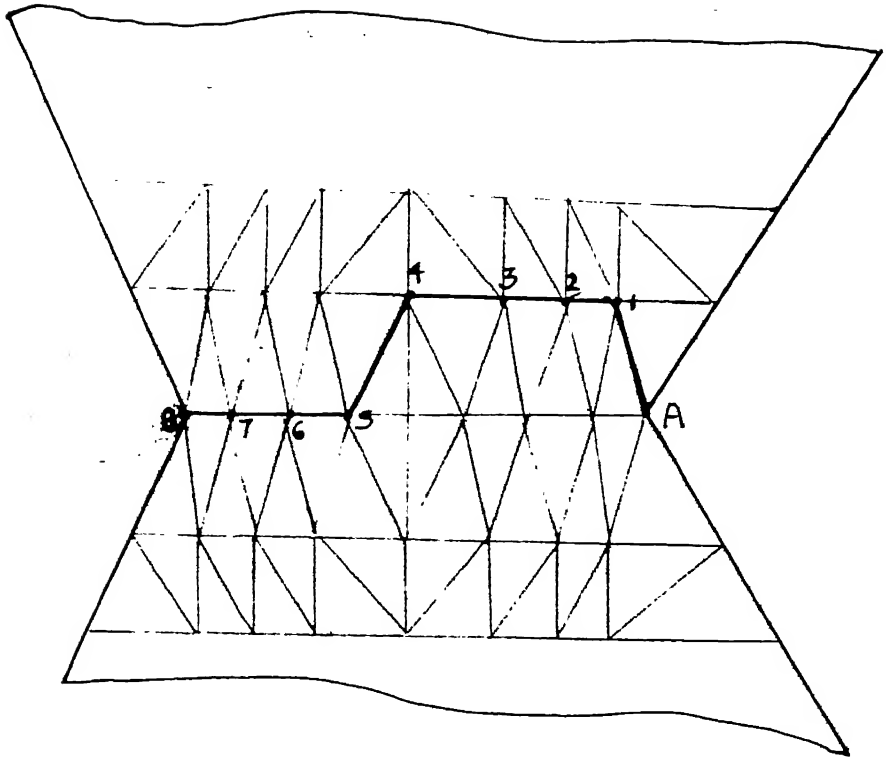

FIG. 4.4 DUCTILE JUNCTION FAILURE

was applied and the check for crack propagation was applied. It was found after successive load increments that at 0.8 P_{ap} crack propagated along one element 1-2 and on checking for further propagation it was seen that 2-3 also cracked. Finally at P_{ap} load the crack propagated from 3 to B along the paths shown. This type of crack propagation is expected in the case of bimetallic junction. When sliding occurs at a bimetallic junction the failure cannot occur in both the bodies simultaneously. It will occur in the weaker of the two bodies. This is a physical observation true for all rubbing bodies.

It was observed that after point 4 (Fig. 4.4) the crack path showed a tendency to fall to the interface. This could be because of the symmetry of the junction being lost due to the opening of the crack. A plot of load applied versus crack length is given in Fig. 4.5.

Crack propagation in the coarse mesh was also analysed and the results are shown in Fig. 4.6. When a junction is formed between two asperities of same materials, the fracture can occur with equal ease in both bodies. Thus the initiation of the fracture must occur simultaneously as already discussed in Section 1.3 . This indeed has been verified by Brockley [13] through his experimental (Figure 1.4). Thus having checked the finite element model for a bimetallic junction and a brittle material-junction the model was applied to analyse a junction of same material.

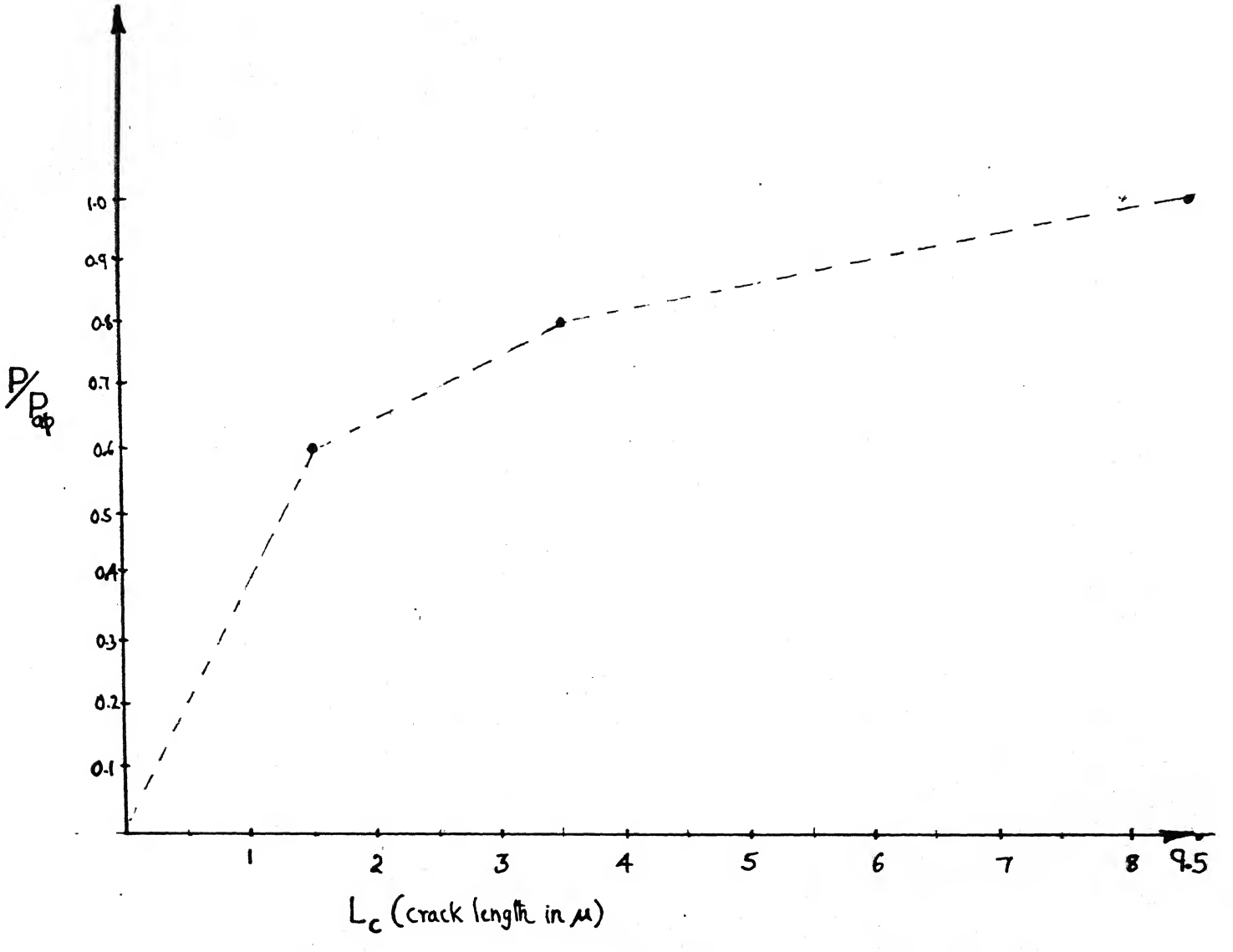

FIG. 4.5 LOAD APPLIED VERSUS CRACK LENGTH

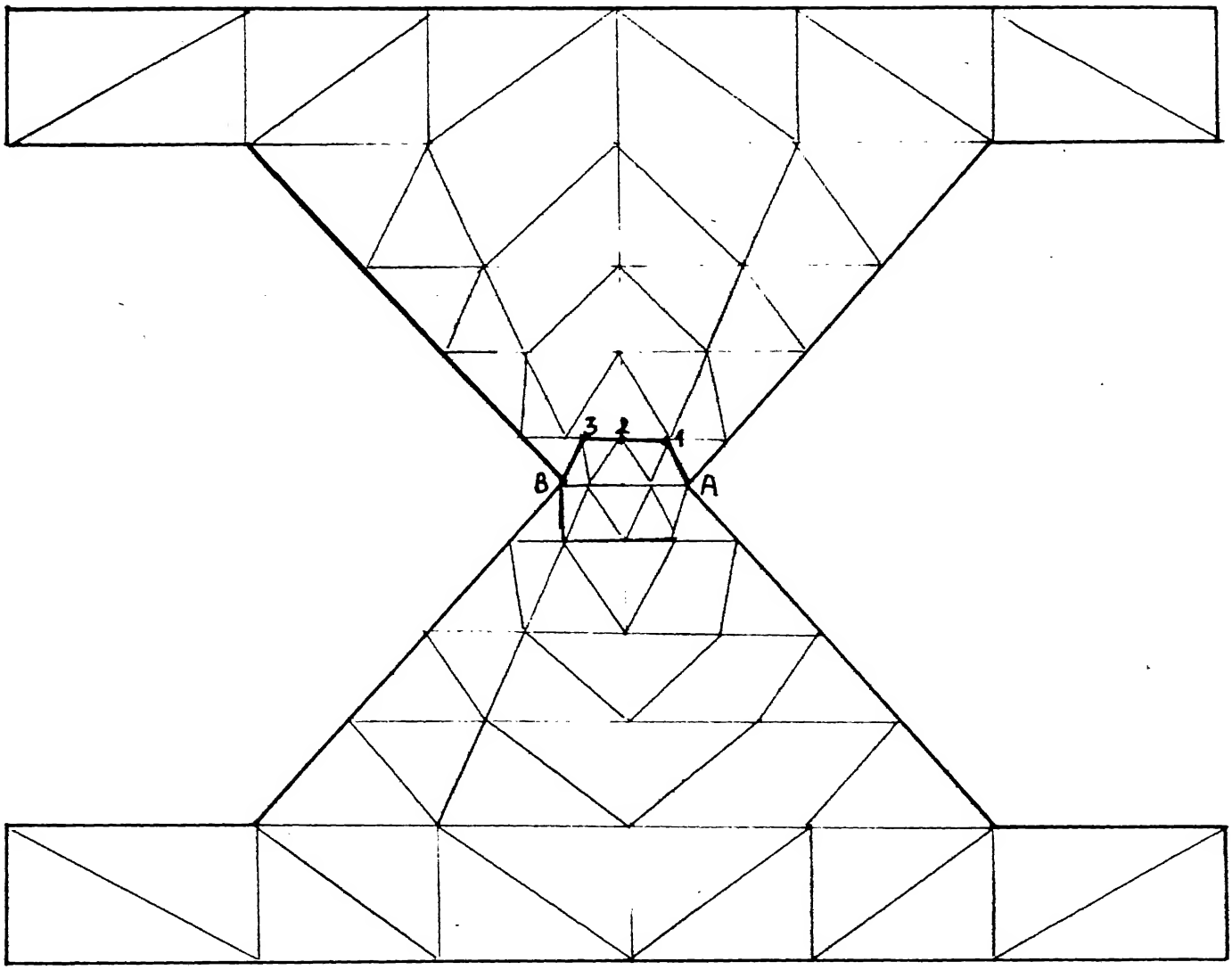

FIG 4.6. DUCTILE JUNCTION FAILURE COARSE MESH

Therefore, fracture path of asperity junction with crack starting from both sides was carried out by incorporating a few changes in the computer code. Here the fracture started in both sides at 0.6 P_{ap}. Again, after first element edge had cracked the crack did not propagate and only at 0.8 P_{ap} crack started propagating from both sides. But it was observed that after crack had propagated along two more element edges it was found that the rate of convergence became very slow and large number of iterations would have been required before the criterion for convergence was satisfied. Hence the analysis was stopped at this stage.

The initiation of cracks from both sides agreed well with the experimental work of Brockley and Fleming [13] where their Figure 1.4 shows that crack follows a path very similar to that as obtained using this analysis (Fig. 4.7). This, thus supported the acceptability of the model suggested in this work.

Tables 4.2a and 4.2b lend support to the obtained results as it can be clearly seen that for bimetallic junction the wear coefficient Z is considerably less than that for similar metal junction. Thus meaning lesser adhesive wear at junction.

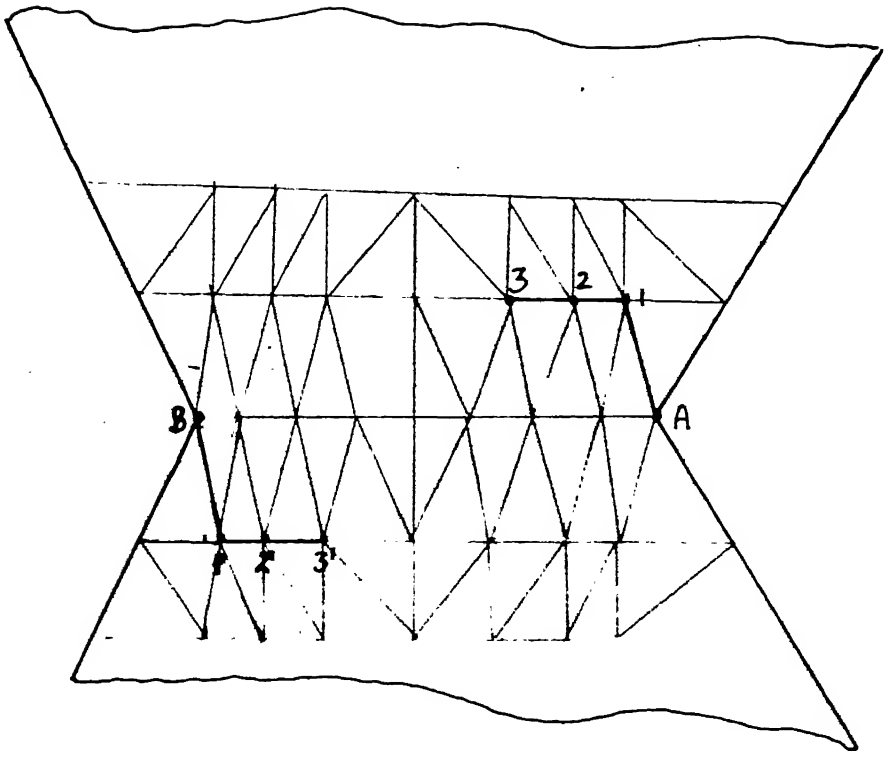

FIG.4.7 UNIMETTALIC JUNCTION FAILURE

TABLE 4.2a [15] Under Identical Conditions

Conditions	Z for metal on metal	
	Similar	Different
Dry surfaces	5×10^{-3}	10^{-3}
Boundary lubrication	2×10^{-4}	10^{-4}
Medium lubrication	10^{-5}	10^{-5}

TABLE 4.2b [15] Under Identical Conditions

Material	Wear coefficient Z
MS/MS	7×10^{-3}
60/40 Brass/MS	$.6 \times 10^{-4}$
70/30 Brass/MS	1.7×10^{-4}

An approximation to the volume of material lost can be made very easily knowing the fracture path as obtained from this analysis.

The broad work is however, far from complete and the model may need to be examined in some detail as outlined in the conclusions chapter.

CHAPTER 5

CONCLUSIONS AND SUGGESTIONS FOR FUTURE WORK

Conclusions:

Based on the results obtained for the proposed model, the following conclusion are drawn:

(i) FE method can be applied to predict the path of fracture at welded asperity junctions.

(ii) The maximum shear stress criteria is acceptable for predicting thepath of fracture.

(iii) The present approach explains fairly well the qualitative behaviour of the fracture of asperity junctions in the case of brittle and ductile materials.

The following are a few of the suggestions which the author feels would be of importance towards the acceptability of the proposed model, as a standard one.

(i) Finer meshes should be tried out to fit the exact path of fracture in the asperity junction.

(ii) Other criterias like energy release rate, stress intensity factors etc. should be investigated to find fracture path.

(iii) The author strongly feels that experimental work using simulated junction models of both brittle and ductile materials should be carried out and some statistical results obtained.

(iv) The application of magnetic field on the fracture path should also be investigated since the influence of magnetic field on wear is fairly well established and the basic mechanisms like change in fracture path is responsible for change in wear characteristics.

(v) The present analysis allows the crack to propagate along the edges of the elements only. More realistic analysis can be modelled by modifying the analysis so that the crack can propagate across the elements also.

REFERENCES

[1] V.Z. Parton and E.M. Morozow, "Elastic-plastic fracture mechanics", Mir-Publishers, Moscow.

[2] P.C. Paris and G. Sih, "Fracture toughness testing and applications", ASTM Special technical publication No. 381, pp. 30-81, Philadelphia (1965).

[3] K. Jerram and T.K. Hellen, "Finite element techniques in fracture mechanics", Proc. of Int. Conference on welding research related to power plants, Southampton (1972).

[4] V.B. Watwood, "The finite element method for prediction of crack behaviour", Nuclear Engineering Design II, pp. 323-332 (1969).

[5] A.A. Griffiths, "The phenomena of flow and rupture in solids", Phil. Trans. Roy. Soc. (Lond.) A221, pp. 163-198.

[6] T.K. Hellen, "On the method of virtual crack extensions", Int. Journal for Numerical Methods in Engg. Vol. 9 (1975), pp. 187-207.

[7] D.M. Parks, "A stiffness derivative of finite element technique for determination of elastic crack tip stress intensity factors, Int. Journal of fracture, 10, pp. 487-502 (1974).

[8] N.P. Suh, "The delamination of wear and the wear of composite surface", Wear, 32 (1975) p. 33.

[9] E.D. Doyle, "A mechanism of spherical particle formation in wear debris", J. Aust. Inst. Metals 19 (1974) p. 276.

[10] F.F. Simpson and R.W. Russel, "Influence of magnetic field and the passage of electrical currents on the deterioration of ball-bearings, Proc. Conf. on Lub. & Wear, London (1975), p. 577.

[11] E. Rabinowicz, "Investigation of size effects in sliding by means of statistical techniques", Inst. Mech. Engrs. Conference on lubrication and wear (1951), p. 10.

[12] A.P. Green, "Friction between unlubricated metals, A Theoretical analysis of the junction mode", Proc. of Roy. Soc. (London), 228 (1955), p.191.

[13] C.A. Brockley, and C.K. Fleming, "A model junction study of severe metallic wear", Wear, 8 (1965) p.374.

[14] A.P. Green, "The plastic yielding of metal junctions due to combined shear and pressure", J. Mech. Phys. Solids 2 (1954), p. 197.

[15] I.V. Kragelskii, "Friction and wear", Butterworths, Washington (1965), p.1.

[16] R. Holm, "Electrical contacts", Almquist and Wiksells, Stockholm, (1948).

[17] F.P. Bowden and D. Tabor, "The friction and lubrication of solids", Oxford University Press, N.Y. (1050).

[18] J. Dyson and W. Hirst, "The true contact area between solids", Proc. Phys. Soc. (London), B67 (1954) p. 309.

[19] I. Ming Feng, "Metal transfer and wear", J. Appl. Phys. 23 (1952) 1011.

[20] F.F. Ling, "On asperity distribution of metal surface", J. Appl. Phys. 29 (1958), p. 1168.

[21] J.A. Green Wood and J.B.P. Williamson, "Contact of nominally flat surfaces", Proc. Roy. Soc. (London), A295 (1966) p. 300.

[22] C.M. Edward and J. Halling, "An analysis of the plastic interaction of surface asperities and its relevance to the coefficient of friction", Mech. Engg. Sci., 10 (1968).

[23] P.K. Gupta and N.H. Cook, "Junction deformation models for asperities in sliding interaction", Wear 20 (1972), p. 73.

[24] O.C. Zienkiewicz, "The finite element method, McGraw Hill Book Company (U.K.) Ltd. 1977.

[25] C. Vijay, "FE analysis of strip and circular plate anchors, Ph.D. Thesis, IIT Kanpur, Feb. 1981.

[26] K.J. Bathe and Wilson, Numerical methods in FE analysis, Prentice Hall India Ltd., 1978.

[27] O.C. Zienkiewicz, S. Valliappan and I.P. King, "Elasto-plastic solutions of Engg. problems using initial-stress, FE approach, Int. Jour. for Num. Methods in Engg., Vol. I, 1969.

[28] Y. Yamada and N. Yoshimura, "Plastic stress-strain matrix and its application for the solution of elastic-plastic problems by FEM", Int. J. Mech. Sci., Vol. 10, 1968, pp. 343-354.

[29] G.C. Nayak and O.C. Zienkiewicz, "A note on alpha constant stiffness matrix for the analysis of non-linear problem, Int. Journal for Num. Methods in Engg", Vol. 4, 1972, pp. 579-82.

[30] N.H. Cook,"Manufacturing analysis", Addison Wesley Publications, 1966.

[31] T.F.J. Quinn, "Division of heat and surface temperatures at sliding steel interface and their relation to oxidational wear, ASLE Preprint 76-LC-10-1.

APPENDIX

A.1

$$N_1 = L_1 (2L_1 - 1)$$
$$N_2 = L_2 (2L_2 - 1)$$
$$N_3 = L_3 (2L_3 - 1) \qquad \text{(REFER [24])}$$
$$N_4 = 4\, L_1 L_2$$
$$N_5 = 4\, L_2 L_3$$
$$N_6 = 4\, L_1 L_3$$

Cartesian co-ordinates x, y and natural co-ordinates L_1, L_2 and L_3 are related as follows:

$$\begin{Bmatrix} 1 \\ x \\ y \end{Bmatrix} = \begin{bmatrix} 1 & 1 & 1 \\ x_1 & x_2 & x_3 \\ y_1 & y_2 & y_3 \end{bmatrix} \begin{Bmatrix} L_1 \\ L_2 \\ L_3 \end{Bmatrix}$$

A.2

$$B = \begin{bmatrix} \frac{\partial N_1}{\partial x} & 0 & \frac{\partial N_2}{\partial x} & 0 & \frac{\partial N_3}{\partial x} & 0 & \frac{\partial N_4}{\partial x} & 0 & \frac{\partial N_5}{\partial x} & 0 & \frac{\partial N_6}{\partial x} & 0 \\ 0 & \frac{\partial N_1}{\partial y} & 0 & \frac{\partial N_2}{\partial y} & 0 & \frac{\partial N_3}{\partial y} & 0 & \frac{\partial N_4}{\partial y} & 0 & \frac{\partial N_5}{\partial y} & 0 & \frac{\partial N_6}{\partial y} \\ \frac{\partial N_1}{\partial y} & \frac{\partial N_1}{\partial x} & \frac{\partial N_2}{\partial y} & \frac{\partial N_2}{\partial x} & \frac{\partial N_3}{\partial y} & \frac{\partial N_3}{\partial x} & \frac{\partial N_4}{\partial y} & \frac{\partial N_4}{\partial x} & \frac{\partial N_5}{\partial y} & \frac{\partial N_5}{\partial x} & \frac{\partial N_6}{\partial y} & \frac{\partial N_6}{\partial x} \end{bmatrix}$$

(REFER [24])

A.3

$$D = \frac{E}{1-\nu^2}\begin{bmatrix} 1 & \nu & 0 \\ \nu & 1 & 0 \\ 0 & 0 & \frac{1-\nu}{2} \end{bmatrix}$$

E = Elastic Modulus

ν = Poissons Ratio

(REFER [24])

A.4

$$[D_p] = \frac{E}{1+\nu}\begin{bmatrix} \left(\frac{1-\nu}{1-2\nu} - \sigma'^2_x\right) & & & & & \\ \left(\frac{\nu}{1-2\nu} - \frac{\sigma'_x\sigma'_y}{S}\right) & \left(\frac{1-\nu}{1-2\nu} - \frac{\sigma'^2_y}{S}\right) & & & & \text{SYMM.} \\ \left(\frac{\nu}{1-2\nu} - \frac{\sigma'_x\sigma'_z}{S}\right) & \left(\frac{\nu}{1-2\nu} - \frac{\sigma'_x\sigma'_z}{S}\right) & \left(\frac{1-\nu}{1-2\nu} - \frac{\sigma'^2_z}{S}\right) & & & \\ \left(\frac{-\sigma'_x\tau_{xy}}{S}\right) & \left(\frac{-\sigma'_y\tau_{xy}}{S}\right) & \left(\frac{-\sigma'_z\tau_{xy}}{S}\right) & \left(\frac{1}{2} - \frac{\tau^2_{xy}}{S}\right) & & \\ \left(\frac{-\sigma'_x\tau_{yz}}{S}\right) & \left(\frac{-\sigma'_y\tau_{yz}}{S}\right) & \left(\frac{-\sigma'_z\tau_{yz}}{S}\right) & \left(\frac{-\tau_{xy}\tau_{yz}}{S}\right) & \left(\frac{1}{2} - \frac{\tau^2_{yz}}{S}\right) & \\ \left(\frac{-\sigma'_x\tau_{zx}}{S}\right) & \left(\frac{-\sigma'_y\tau_{zx}}{S}\right) & \left(\frac{-\sigma'_z\tau_{zx}}{S}\right) & \left(\frac{-\tau_{xy}\tau_{zx}}{S}\right) & \left(\frac{-\tau_{yz}\tau_{zx}}{S}\right) & \left(\frac{1}{2} - \frac{\tau^2_{zx}}{S}\right) \end{bmatrix}$$

(REFER [28])

E = Elastic modulus

ν = Poisson's Ratio

$S = \frac{2}{3}\bar{\sigma}^{-2}\left(1 + \frac{H'}{3G}\right)$

$\bar{\sigma} = \frac{1}{\sqrt{2}}[(\sigma_x - \sigma_y)^2 (\sigma_y - \sigma_z)^2 + (\sigma_z - \sigma_x)^2 + 6(\tau^2_{xy} + \tau^2_{zy} + \tau^2_{zx})]^{1/2}$

G = Shear modulus

H' = Strain hardening parameter